Available online at www.sciencedirect.com
ScienceDirect
Coordination Chemistry Reviews 250 (2006) 2194–2211
COORDINATION CHEMISTRY REVIEWS
www.elsevier.com/locate/ccr

Review

Magnetic interactions in one-, two-, and three-dimensional assemblies of dinuclear ruthenium carboxylates

Masahiro Mikuriya [a,*], Daisuke Yoshioka [a], Makoto Handa [b,*]

[a] *Department of Chemistry and Open Research Center for Coordination Molecule-Based Devices, School of Science and Technology, Kwansei Gakuin University, Sanda, Hyogo 669-1337, Japan*
[b] *Department of Material Science, Interdisciplinary Faculty of Science and Engineering, Shimane University, Matsue, Shimane 690-8504, Japan*

Received 28 September 2005; accepted 16 January 2006
Available online 24 February 2006

Contents

Abstract

Dinuclear ruthenium complexes which have metal–metal bonds within a paddlewheel dinuclear core are currently recognized, because of their unique magnetic properties, as one of the more interesting building blocks with which to construct metal-assembled complexes. The use of dinuclear ruthenium units such as ruthenium carboxylates has been explored toward molecular assemblies using a variety of linking ligands. In this review, recent examples of assembled complexes of dinuclear ruthenium carboxylates with *N*,*N*′-bidentate ligands (pyrazine, 4,4′-bipyridine, 1,4-diazabicyclo[2.2.2]octane, phenazine, tetramethylpyrazine), *p*-quinones (1,4-benzoquinone, 1,4-naphthoquinone, 9,10-anthraquinone), organic electron acceptors with cyano groups (tetracyanoethylene, 7,7,8,8-tetracyanoquinodimethane, and 2,5-dimethyl-*N*,*N*′-dicyanobenzoquinonediimine), nitroxide radicals (2,2,6,6-tetramethylpiperidine-1-oxyl, 2-phenyl-4,4,5,5-tetramethyl-4,5-dihydro-1*H*-imidazolyl-1-oxyl 3-*N*-oxide, 2,4,4,5,5-pentamethyl-4,5-dihydro-1*H*-imidazol-1-oxyl 3-*N*-oxide, 2-ethyl-4,4,5,5-tetramethyl-4,5-dihydro-1*H*-imidazol-1-oxyl 3-*N*-oxide, 2-(4-pyridyl)-4,4,5,5-tetramethyl-4,5-dihydro-1*H*-imidazolyl-1-oxyl 3-*N*-oxide, 2-(3-pyridyl)-4,4,5,5-tetramethyl-4,5-dihydro-1*H*-imidazolyl-1-oxyl 3-*N*-oxide), and inorganic hexacyanometalate(III) ions are discussed in relation to the assembled structures and the magnetic properties.

Keywords: Ruthenium; Carboxylate; Dinuclear complex; Magnetism

1. Introduction

Dinuclear ruthenium carboxylates with a paddlewheel structure have been subjected to intensive study for the past three decades because of their unique properties [1]. In the mid 1960s, it was discovered by Stephenson and Wilkinson that ruthenium can form dinuclear carboxylate species with metal–metal interaction [2]. A similar ruthenium formate was reported by Mukaida et al. soon after this observation [3]. To date, there have been a number of reports dealing with ruthenium carboxylates. These dinuclear carboxylates have a ‘paddlewheel’ dinuclear core (Scheme 1) which was originally found in copper(II) acetate as the so-called lantern-type dinuclear complexes in 1953 [4,5]. The paddlewheel core in the dinuclear ruthenium carboxylates

* Corresponding authors. Tel.: +81 79 565 8365; fax: +81 79 565 9077.
E-mail address: junpei@ksc.kwansei.ac.jp (M. Mikuriya).

0010-8545/$ – see front matter © 2006 Elsevier B.V. All rights reserved.
doi:10.1016/j.ccr.2006.01.011

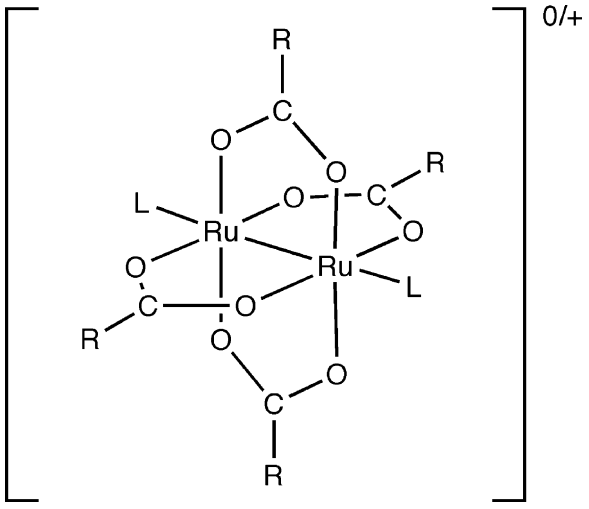

Scheme 1. Ruthenium carboxylates with a paddlewheel dinuclear core.

was confirmed by Cotton and co-workers for the first time as a chain-like polymeric structure with an alternated arrangement of the dinuclear units and chloride ions in the crystal structure of $[Ru_2(O_2CC_3H_7)_4Cl]_n$ [6]. The paddlewheel dinuclear core is a very useful building unit to design one-dimensional chain molecules. The axial sites are usually labile and available for molecular assembly using linking ligands. The unique property of the ruthenium carboxylates is that the mixed-valent $Ru_2^{II,III}$ oxidation state is relatively stable and exists in a variety of carboxylates and other metal–metal bonded dinuclear species. On the other hand, the neutral $Ru_2^{II,II}$ carboxylates are generally air-sensitive and more difficult to synthesize. The first successful synthesis of such a species was accomplished by Wilkinson and co-workers only 20 years ago [7–9]. While the $[Ru_2^{II,II}(O_2CR)_4]$ state has two unpaired electrons, the $[Ru_2^{II,III}(O_2CR)_4]^+$ state has three unpaired electrons in the metal–metal bond manifold due to an accidental near-degeneracy of the two highest lying occupied π^* and δ^* molecular orbitals [10,11]. This higher spin state of three unpaired electrons ($S = 3/2$) can be incorporated into a spin source of new magnetic materials. A useful review covering a wide range of dinuclear ruthenium carboxylate chemistry was reported by Aquino [12]. After this, some review articles on ruthenium carboxylates including Aquino's second review which is the update of the literature through 2003, appeared [13–15]. Cotton, Murillo, and Walton's textbook on metal–metal bond compounds deals with diruthenium chemistry giving us essential background [1].

There have been more than 80 reports of single-crystal X-ray diffraction studies on ruthenium(II, III) carboxylates of formula $Ru_2(O_2CR)_4L_nX_m$ (R = alkyl and aryl; L = neutral ligand; X = monoanion; $n = 0$, 1/2, 1, 2; $m = 0$, 1, 2), since the first crystal structure report on the chloro complex of ruthenium(II, III) butyrate [6]. These structures can be divided into six types: (a) di-adducts with two neutral ligands, (b) di-adducts of neutral and monoanionic ligands, (c) di-adducts with two anionic ligands, (d) linear or bent chain compounds where the Ru_2 cores are bridged by monoanionic ligands, (e) linear or bent chain compounds where the Ru_2 cores are bridged by neutral ligands, and (f) linear or bent tetranuclear (dimer-of-dimers) compounds in which the two Ru_2 cores are bridged by a neutral ligand (Scheme 2). The X-ray crystallographic data show that the structural parameters of the $Ru_2^{II,III}$ cores vary only to a small degree with the bridging carboxylate and the axial ligand: the Ru–Ru bond lengths range from 2.248(1) to 2.310(2) Å except for the case of $[Ru_2(O_2CCH_3)_4(tcp)_2]PF_6$ (tcp = tris(cyclohexyl)phosphine) [Ru–Ru 2.427(1) Å] [16]. Interestingly, the $Ru_2^{II,II}$ cores have an almost similar size to those of the $Ru_2^{II,III}$ cores: the Ru–Ru bond lengths [2.252(2)–2.311(1) Å] show only a small increase in length except for $[Ru_2(O_2CCF_3)_4(NO)_2]$ [Ru–Ru 2.532(4) Å] and $[Ru_2(O_2CC_2H_5)_4(NO)_2]$ [Ru–Ru 2.515(4) Å][9]. This can be explained by the small effect of the population/depopulation of a δ^* orbital on the Ru–Ru bond length, which is compensated for by the decrease/increase in the electrostatic repulsion between the metals [12]. A series of ruthenium(II, III) carboxylates $[Ru_2(O_2CR)_4X]$ and $[Ru_2(O_2CR)_4(H_2O)X]$ ($R = CH_2CH_2OC_6H_5$, $C(C_6H_5)_2CH_3$, C_6H_5, C_6H_4-*p*-CH_3; $X = Cl^-$, Br^-, I^-), were studied by Jimenez-Aparicio and co-workers [17,18]. Based on X-ray crystallographic data types (b) and (d) structures could be seen for most of these systems, while $[Ru_2(O_2CCH_2CH_2OC_6H_5)_4(H_2O)I]$ was found to be actually $[Ru_2(O_2CCH_2CH_2OC_6H_5)_4(H_2O)_2][Ru_2(O_2CCH_2CH_2OC_6H_5)_4I_2]$ (types (a) and (c)). The crystal structure of $[Ru_2(O_2CCH_3)_4(H_2O)(NO_3)]$ with type (b) structure was reported [19]. Homoleptic diruthenium(II, III) trifluoroacetate, $Ru_2(O_2CCF_3)_5$, has a zig-zag chain structure where the $Ru_2^{II,III}(O_2CCF_3)_4$ units and μ-O_2CCF_3-*O*,*O*′-bridges are arranged alternately [20]. Dikarev and Li found a disproportionation reaction of this complex in acetone, $4Ru_2^{II,III} \rightarrow 2Ru_3^{II,III,III} + Ru_2^{II,II}$ [21]. They reported an interesting crystal structure of the isolated complex $[Ru_3O(O_2CCF_3)_6((CH_3)_2CO)_3]_2[Ru_2(O_2CCF_3)_4((CH_3)_2CO)_2]$ containing the acetone adducts of μ_3-oxo-trinuclear ruthenium trifluoroacetate and dinuclear ruthenium trifluoroacetate cocrystallized in a 2:1 ratio. Cukiernik and co-workers continued their study on the mesomorphic properties of ruthenium(II, III) carboxylates and reported the liquid-crystalline properties of $[Ru_2(O_2C(CH_2)_{n-2}CH_3)_4X]$ (X = dodecylsulfate, $n = 8$, 9, 16, and 18; X = octylsulfonate, $n = 8$, 10, 12, 14, and 18) [22]. With respect to ruthenium(II, II) carboxylates, the crystal structure of bis-adduct $[Ru_2(O_2CCH_3)_4L_2]$ (L = *N*,*N*′-di-*p*-anisylformamidine) was reported [23].

2. One-dimensional assemblies

2.1. *N*,*N*′-Bidentate ligands

It is well known that *N*,*N*′-bidentate ligands such as pyrazine (Scheme 3) work as linking ligands to connect metal units in an axially bidentate fashion to form one-dimensional chain compounds. These organic ligands generally have a rigid framework and good direction toward linearity to form an one-dimensional array (type (e), Scheme 2). The first attempt to construct an one-dimensional chain was done by the use of pyrazine for

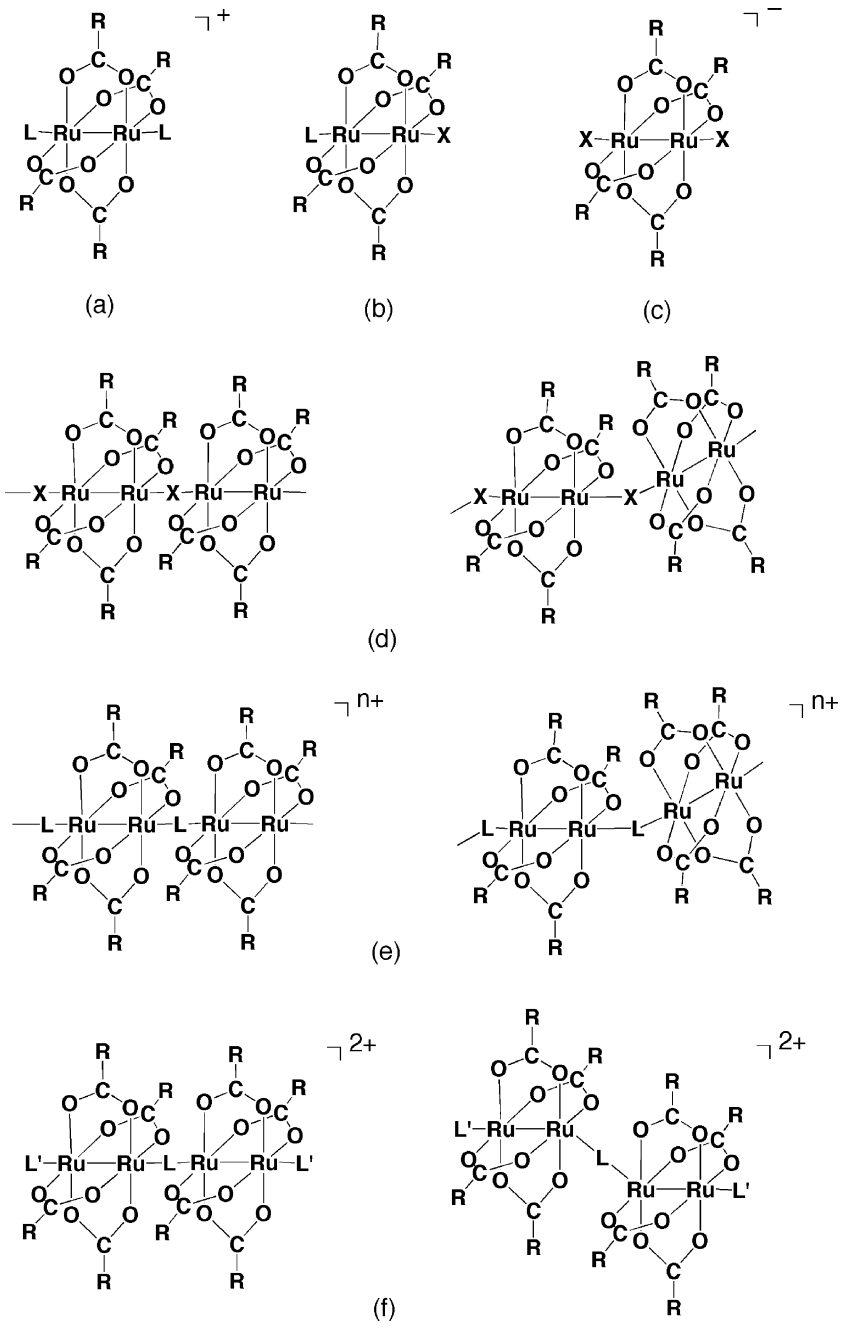

Scheme 2. Structural types of ruthenium(II, III) carboxylates.

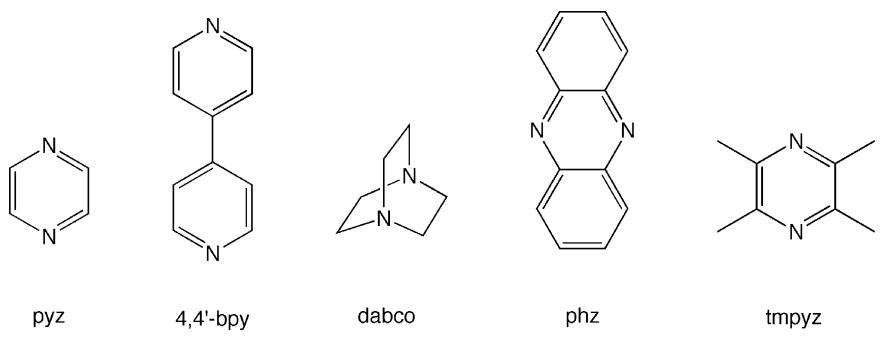

Scheme 3. Structural formulae of *N*,*N*′-bidentate ligands.

copper(II) acetate [24,25]. An earlier study was reported by Cotton et al. [26]. They used an aromatic diamine, phenazine (phz), as the linking ligand to obtain a chain compound of ruthenium(II, III) propionate $[Ru_2(O_2CC_2H_5)_4(phz)]_n(BF_4)_n$. Crystallographic study shows that the Ru–Ru–N angles are not linear [168.1(1)° and 176.2(1)°], causing the zig-zag chain structure of type (e). The magnetic susceptibility data suggest that an antiferromagnetic interaction between the 3/2 spins of the dinuclear ruthenium units proceeds through the phenazine bridges in addition to the zero-field splitting of the dinuclear units. A more detailed study of the magnetic properties of this type of complex was performed for chain complexes of ruthenium(II, III) acetate with pyrazine (pyz), 4,4′-bipyridine (4,4′-bpy) and 1,4-diazabicyclo[2.2.2]octane (dabco) by Cukiernik et al. [27] and Aquino and co-workers [28]. They adopted a molecular field approximation as has been treated by Telser and Drago [29] referring to the O'Connor's review [30]:

$$\chi' = \chi/\{1 - (2zJ/Ng^2\mu_B^2)\chi\}, \quad (1)$$

where zJ is the exchange energy multiplied by the number of interacting neighbors, and χ is the magnetic susceptibility of an isolated molecule:

$$\chi = (1-p)[(\chi_\parallel + 2\chi_\perp)/3 + \text{tip}] + pN\mu_B^2 g_{\text{mono}}^2/4kT. \quad (2)$$

here, $\chi_\parallel$ and $\chi_\perp$ are magnetic susceptibility terms defined as follows:

$$\chi_\parallel = (Ng^2\mu_B^2/kT)[1 + 9\exp(-2D/kT)]/4\{1 + \exp(-2D/kT)\}, \quad (3)$$

$$\chi_\perp = (Ng^2\mu_B^2/kT)[4 + (3kT/D)\{1 - \exp(-2D/kT)\}]/4\{1 + \exp(-2D/kT)\}, \quad (4)$$

where D is the zero-field splitting parameter.

Eq. (2) includes correction terms for temperature-independent paramagnetism (tip) and a small amount (p) of paramagnetic impurity (usually a mononuclear Ru^{III} species ($S = 1/2$) with a g factor, noted as here g_{mono}).

The parameters determined from fitting Eq. (1) for the magnetic data of $[Ru_2(O_2CCH_3)_4L]_nX_n$, where L = pyz, 4,4′-bpy, and dabco; X = BPh_4^- and PF_6^- (BPh_4^- = tetraphenylborate ion, PF_6^- = hexafluorophosphate ion) are listed together with those of other ruthenium carboxylates in Table 1. Non-negligible interdimer interactions were observed; the four complexes have zJ values of −2.3, −1.0, −0.65, and −0.59 cm^{-1}, respectively. We further worked on this system by using a variety of *N*,*N*′-bidentate ligands, pyz, 4,4′-bpy, dabco, phenazine (phz), and tetramethylpyrazine (tmpyz) for ruthenium(II, III) pivalate [31]. We obtained chain complexes $[Ru_2(O_2CC(CH_3)_3)_4L]_n(BF_4)_n$ (where L is pyz, 4,4′-bpy, dabco, or phz) and $[Ru_2(O_2CC(CH_3)_3)_4(H_2O)_2(tmpyz)]_n(BF_4)_n$, and a tetranuclear complex $[\{Ru_2(O_2CC(CH_3)_3)_4(H_2O)\}_2(phz)](BF_4)_2$. These complexes are antiferromagnetic. These complexes were analyzed using Eq. (1) and the results reported. However, the reported fit was rather poor in the low-temperature region for some compounds, and hence the analysis was repeated using

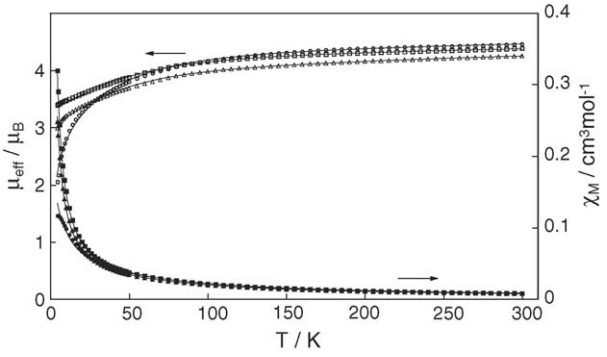

Fig. 1. Temperature dependence of magnetic susceptibilities (●, ▲, ■) and effective magnetic moments of (◯, △, □) of $[Ru_2(O_2CC(CH_3)_3)_4(pyz)]_n(BF_4)_n$ $[Ru_2(O_2CC(CH_3)_3)_4(4,4'\text{-bpy})]_n(BF_4)_n$ and $[Ru_2(O_2CC(CH_3)_3)_4(dabco)]_n(BF_4)_n$. The solid lines show the best fit obtained.

Eq. (1) to give a better fit as shown in Figs. 1 and 2; the six complexes have zJ values of −3.12, −0.45, −0.01, −1.47, −0.09, and −0.65 cm^{-1}, respectively. The g and D values obtained for these complexes are similar to those reported previously for mixed-valent diruthenium carboxylates (Table 1). The antiferromagnetic interaction between the $Ru_2^{II,III}$ units through the linking ligand become stronger (more negative in J value) in the order of dabco < tmpyz ∼ tcnq (7,7,8,8-tetracyanoquinodimethane) ∼ dmdcnqi (2,5-dimethyl-*N*,*N*′-dicyanobenzoquinonediimine) ∼ $C(CN)_3^-$ ∼ $N(CN)_2^-$ < 4,4′-bpy < phz < pyz. The interdimer antiferromagnetic interaction for the pyrazine-bridged complexes is significantly greater than those observed for the other compounds. For the 4,4′-bpy, tcnq, dmdcnqi, $C(CN)_3^-$, and $N(CN)_2^-$ complexes, the large separation between the two Ru_2 cores is most probably the main reason for the weaker magnetic interaction. In the case of the phz complex, it is reasonable to assume a similar situation to the 4,4′-bpy complex, because of the rather weak coordination of the phz molecule. The dabco complexes exhibit the least interaction among these complexes. The dabco molecule does not have any π-pathway, because it has only a σ bond system. It seems reasonable to conclude that pyrazine mediates an antiferromagnetic interaction most efficiently by using the π system. In the cases of halogeno carboxylates $[Ru_2(O_2CR)_4X]$

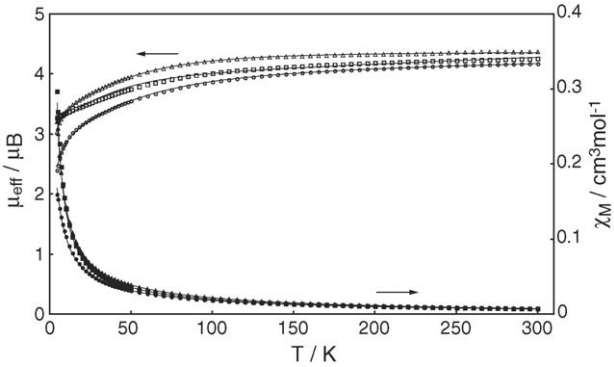

Fig. 2. Temperature dependence of magnetic susceptibilities (●, ▲, ■) and effective magnetic moments of (◯, △, □) of $[Ru_2(O_2CC(CH_3)_3)_4(phz)]_n(BF_4)_n$ $[\{Ru_2(O_2CC(CH_3)_3)_4(H_2O)\}_2(phz)](BF_4)_2$, and $[Ru_2(O_2CC(CH_3)_3)_4(H_2O)_2(tmpyz)]_n(BF_4)_n$. The solid lines show the best fit obtained.

Table 1
Magnetic parameters of ruthenium carboxylate compounds

Complex	g	D (cm^{-1})	zJ (cm^{-1})	Ru–X–Ru (°)	References
$Ru_2^{II,III}$ complexes					
$[Ru_2(O_2CCH_3)_4(H_2O)_2]BPh_4$	2.190	71.8	0		[27]
$[Ru_2(O_2CC(CH_3)_3)_4(H_2O)_2]BF_4$	2.15	60	0		[34]
$K_3[Ru_2(hedp)_2(H_2O)_2]$	2.26	96.0	−0.007		[48]
$[Ru_2(O_2CCH_2CH_2OC_6H_5)_4Cl(H_2O)]$	2.00	64.03	−1.33		[17]
$[Ru_2(O_2CC(C_6H_5)_2CH_3)_4Cl(H_2O)]$	2.15	50.60	−0.07		[17]
$[Ru_2(O_2CC(C_6H_5)_2CH_3)_4Br(H_2O)]$	2.09	62.80	−0.08		[17]
$[Ru_2(O_2CC_6H_4$-p-$OCH_3)_4Br(H_2O)]$	2.30	70.0	−0.04		[18]
$[Ru_2(O_2CC(C_6H_5)_2CH_3)_4I(H_2O)]$	2.02	62.80	−0.20		[17]
$[Ru_2(O_2CCH_2CH_2OC_6H_5)_4I(H_2O)]$	2.02	64.72	−0.04		[17]
$[Ru_2(O_2CC_6H_4$-p-$OCH_3)_4I(H_2O)]$	2.35	70.0	−0.04		[18]
$[Ru_2(O_2CCH(CH_3)_2)_4Cl(thf)]$	2.07	61.7	−0.09		[35,39]
$[Ru_2(O_2CC(CH_3)_3)_4Cl(H_2O)]$	2.04	65.2	−0.09		[35,39]
$[Ru_2(O_2CC_4H_4N)_4Cl(thf)]$	2.21	68.1	−0.13		[35,40]
$[Ru_2(O_2CCH_3)_4(NO_3)(H_2O)]$	2.23	94	−4.91		[19]
$[Ru_2(O_2CC_6H_5)_4(H_2O)_2][Ru_2(O_2CC_6H_5)_4(ReO_4)_2]$	2.06	50.00	−0.07		[46]
$(C_4H_9)_4N[Ru_2(O_2CC_6H_5)_4(ReO_4)_2]$	2.10	53.84	−0.04		[46]
$[Ru_2(O_2CCH_3)_4Cl]_n$ (**1**)	2.07[a]	54	0	127.6	[33,36]
	2.17[a]	75	−0.19		[33]
$[Ru_2(O_2CC_2H_5)_4Cl]_n$ (**2**)	1.90	46.7	−8.05	180	[32,37]
$[Ru_2(O_2CC_3H_7)_4Cl]_n$ (**3**)	2.10	70.6	0	125.4	[29,6,33]
	2.21[a]	69	0		[33]
$[Ru_2(O_2CC_4H_9)_4Cl]_n$ (**4**)	2.12[a]	67	−4.6	142.3(1)	[33]
$[Ru_2(O_2CC_7H_{15})_4Cl]_n$	2.18[a]	80	−0.9		[33]
$[Ru_2(O_2CC_8H_{17})_4Cl]_n$	2.26[a]	75	−0.9		[33]
$[Ru_2(O_2CC_6H_3(O(CH_2)_{11}CH_3)_2)_4Cl]_n$	2.12	73	−2.4		[33]
$[Ru_2(O_2CC_6H_3(O(CH_2)_{15}CH_3)_2)_4Cl]_n$	2.29	76	−3.2		[33]
$[Ru_2(O_2CC_6H_2(OCH_3)_3)_4Cl]_n$	2.23[a]	64	0.00		[33]
$[Ru_2(O_2C(CH{=}CH)_2CH_3)_4Cl]_n$ (**5**)	2.16	53.9	−2.84	119.43(4)	[35]
$[Ru_2(O_2CCH_2OCH_3)_4Cl]_n$ (**6**)	2.07	67.5	−0.69	110.11(7)	[35]
$[Ru_2(O_2CC(C_6H_5)_2CH_3)_4Cl]_n$ (**7**)	2.06	38.1	−13.28	180	[32,38]
$[Ru_2(O_2CC(CH_3){=}CHC_2H_5)_4Cl]_n$ (**8**)	2.04	48.0	−7.46	180	[32,41]
$[Ru_2(O_2CC_6H_5)_4Br]_n$ (**9**)	2.16	63.4	−1.37	117.00(3)	[18]
$[Ru_2(O_2CCH_2CH_2OC_6H_5)_4Br]_n$	2.00	62.99	−9.08		[17]
$[Ru_2(O_2CC_6H_5)_4I]_n$	2.15	71.5	−0.03		[18]
$Na_{4n}[Ru_2(hedp)_2Cl]_n$ (**10**)	2.1	78.3	−4.6	178.45(5)	[48]
$Na_{4n}[Ru_2(hedp)_2Br]_n$ (**11**)	2.1	92.1	−4.9	178.38(5)	[48]
$[Ru_2(O_2CC_5H_{11})_5]_n$	2.30[a]	60	−3.1		[33]
$[Ru_2(O_2CC_7H_{15})_5]_n$	2.20[a]	78	−1.5		[33]
$[Ru_2(O_2CC_8H_{17})_5]_n$	2.32	70	−3.2		[33]
$[Ru_2(O_2CC_{11}H_{23})_5]_n$	2.20[a]	72	−1.7		[33]
$[Ru_2(O_2CC_{13}H_{27})_5]_n$	2.33	94	−2.4		[33]
$[Ru_2(O_2CC_{15}H_{31})_5]_n$	2.20[a]	71	−1.7		[33]
$[Ru_2(O_2CC_{15}H_{31})_4(dos)]_n$	2.18[a]	72	−0.21		[33]
$[Ru_2(O_2CC(CH_3)_3)_4(H_2O)_2(tmpyz)]_n(BF_4)_n$	2.27[b]	50[b]	−0.09[b]		[31]
$[Ru_2(O_2CC(CH_3)_3)_4(dabco)]_n(BF_4)_n$	2.30[b]	60[b]	−0.01[b]		[31]
$[Ru_2(O_2CCH_3)_4(dabco)]_n(PF_6)_n$	2.096	65.6	−0.593(1)		[28]
$[\{Ru_2(O_2CC(CH_3)_3)_4(H_2O)\}_2(9,10\text{-aq})](BF_4)_2$	2.1	70	0		[42]
$[\{Ru_2(O_2CC(CH_3)_3)_4(H_2O)\}_2(tcnq)](BF_4)_2$	2.10	65	−0.15		[43]
$[Ru_2(O_2CC(CH_3)_3)_4(dmdcnqi)]_n(BF_4)_n$	2.1	20	−0.30		[44]
$[Ru_2(O_2CCH_3)_4(C(CN)_3)]_n$	2.15	58.0	−0.22		[45]
$[Ru_2(O_2CCF_3)_4(N(CN)_2)]_n$	2.16	63.3	−0.33		[45]
$[Ru_2(O_2CCH_3)_4(4,4'\text{-bpy})]_n(PF_6)_n$	2.073	69.7	−0.996(1)		[28]
$[Ru_2(O_2CCH_3)_4(4,4'\text{-bpy})]_n(BPh_4)_n$	2.062	63.1	−0.653(1)		[28]
$[Ru_2(O_2CC(CH_3)_3)_4(4,4'\text{-bpy})]_n(BF_4)_n$	2.13[b]	45[b]	−0.45[b]		[31]
$[Ru_2(O_2CC(CH_3)_3)_4(phz)]_n(BF_4)_n$	2.10[b]	70[b]	−1.47[b]		[31]
$[\{Ru_2(O_2CC(CH_3)_3)_4(H_2O)\}_2(phz)](BF_4)_2$	2.39[b]	65[b]	−0.65[b]		[31]
$[Ru_2(O_2CCH_3)_4(pyz)]_n(BPh_4)_n$	2.098	62.9	−2.3		[27]
$[Ru_2(O_2CC(CH_3)_3)_4(pyz)]_n(BF_4)_n$	2.27[b]	50[b]	−3.12[b]		[31]
$[Ru_2(O_2CCH_3)_4(ReO_4)]_n$	2.18	50.86	−1.74		[46]
$[Ru_2(O_2CC(C_6H_5)_2CH_3)_4(ReO_4)]_n$	2.21	50.03	−1.38		[46]
$[Ru_2(O_2CC(CH_3)_3)_4(ReO_4)]_n$	2.12	53.32	−1.38		[46]
$[Ru_2(O_2CCH_2CH_2OCH_3)_4(ReO_4)]_n$	2.08	63.29	−0.38		[46]

Table 1 (*Continued*)

Complex	g	D (cm^{-1})	zJ (cm^{-1})	Ru–X–Ru (°)	References
$[Ru_2(O_2CC(CH_3)=CHC_2H_5)_4(ReO_4)]_n$	2.31	77.13	−0.74		[46]
$[Ru_2(O_2CC_6H_4\text{-}p\text{-}OCH_3)_4(ReO_4)]_n$	2.06	42.23	−0.18		[46]
$[Ru_2(O_2CC_6H_5)_4(ReO_4)]_n$	2.14	58.98	−0.07		[46]
$Na_{7n}[Ru_2(hedp)_2Fe(CN)_6]_n$	2.30	101.6	−0.044		[48]
$(NH_4)_{3n}[Ru_2(hedp)_2]_n$	2.25	89.4	0.72[c] (25 < T < 300 K)		[47]
$[\{Ru_2(O_2CCH_3)_4\}_3Co(CN)_6]_n$	2.04	69.4	0[c] (4 < T < 300 K)		[49]
$[\{Ru_2(O_2CCH_3)_4\}_3Fe(CN)_6]_n$	2.0	69.4	0[c] (15 < T < 300 K)		[49]
$[\{Ru_2(O_2CCH_3)_4\}_3Mn(CN)_6]_n$	2.0	69.4	−20[c] (60 < T < 300 K)		[49]
$[\{Ru_2(O_2CCH_3)_4\}_3Cr(CN)_6]_n$	2	69.4	−40[c] (120 < T < 300 K)		[49]
$[\{Ru_2(O_2CCH_3)_4\}_3Cr(CN)_6]_n\cdot 1.8nCH_3CN$	2	69.4	−70[c] (120 < T < 300 K)		[49]
$[\{Ru_2(O_2CC(CH_3)_3)_4\}_3Co(CN)_6]_n$	2.04	69.4	0[c] (4 < T < 300 K)		[50]
$[\{Ru_2(O_2CC(CH_3)_3)_4\}_3Fe(CN)_6]_n$	2.04	69.4	−5[c] (50 < T < 300 K)		[50]
$[\{Ru_2(O_2CC(CH_3)_3)_4\}_3Cr(CN)_6]_n$	2.04	69.4	−45[c] (150 < T < 300 K)		[50]
$Ru_2^{II,II}$ complexes					
$[Ru_2(O_2CCH_3)_4(dabco)]_n$	2.19	260	0		[51]
	2.22	260	−3[d]		
$[Ru_2(O_2CCH_3)_4(4,4'\text{-bpy})]_n$	2.15	270	0		[51]
	2.18	270	−3[d]		
$[Ru_2(O_2CCH_3)_4(pyz)]_n$	2.19	290	0		[51]
	2.21	290	−3[d]		
$[Ru_2(O_2CCF_3)_4(phz)]_n$	2.0	277	−3.0		[52]
$[\{Ru_2(O_2CC_6H_5)_4\}_3(trz)_2]_n$	2.0	254	−2.2		[53]

[a] Mean value calculated from $g = (g_{\parallel} + 2g_{\perp})/3$.
[b] Revised data for the reported values [31] (see text).
[c] θ value in Eq. (5).
[d] Another fitting result (see text).

($X = Cl^-, Br^-, I^-$) and homoleptic carboxylates $[Ru_2(O_2CR)_5]$, there was confusion in the magnetic data, showing a wide range of the zJ values (Table 1). Jimenez-Aparicio et al. developed the magnetic susceptibility calculation models for linear chains of $S = 3/2$ ($Ru_2^{II,III}$) units having both a strong antiferromagnetic coupling and a large zero-field splitting which could not be interpreted by the molecular field approximation and applied their methods to the magnetic data of $[Ru_2(O_2CR)_4Cl]$ ($R = C_2H_5$, $C(CH_3)=CHC_2H_5$, $C(C_6H_5)_2CH_3$) [32]. It was pointed out by Cukiernik et al. that the antiferromagnetic interaction between the $Ru_2^{II,III}$ units is the strongest when the Ru–X–Ru angle is 180°, decreases as this angle becomes smaller, and becomes zero for the angle of 125° [33]. In Fig. 3, the zJ values are plotted against the Ru–X–Ru angles. We can see such a relationship between them and this is understandable if we consider the total overlap between the π^* orbitals of the $Ru_2^{II,III}$ cores and the p orbitals of the halogeno bridges [33].

Interestingly, a reaction of $[Ru_2(O_2CC(CH_3)_3)_4(H_2O)_2]BF_4$ with phenazine at room temperature gave a tetranuclear complex with a "dimer-of-dimers" structure (type (f), Scheme 2) $[\{Ru_2(O_2CC(CH_3)_3)_4(H_2O)\}_2(phz)](BF_4)_2$ (Fig. 4) [31]. When the same reaction was carried out in benzene heated to reflux, a polynuclear chain complex (type (e)) $[Ru_2(O_2CC(CH_3)_3)_4(phz)]_n(BF_4)_n$ was isolated in a good yield. Heating is necessary to obtain this chain compound, possibly because of the weak linking nature of phenazine.

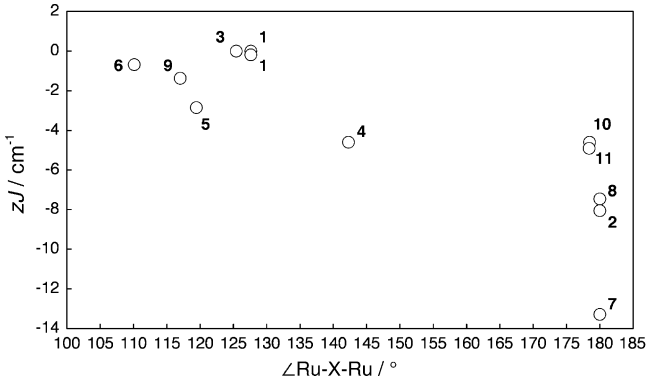

Fig. 3. Plots of the experimental zJ values vs. Ru–X–Ru bond angles. Numbers refer to the complexes listed in Table 1.

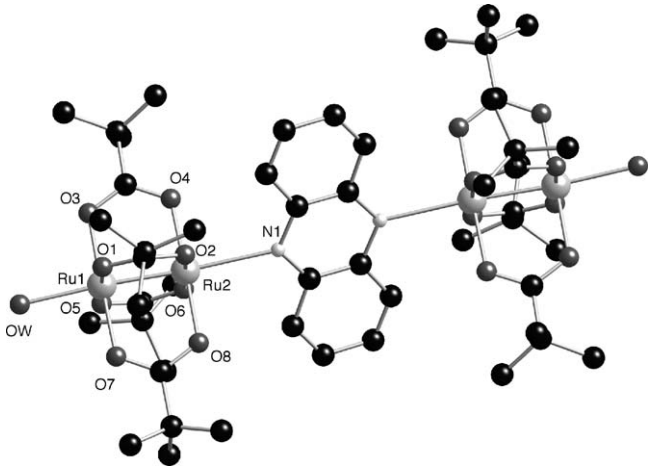

Fig. 4. Crystal structure of the $[\{Ru_2(O_2CC(CH_3)_3)_4(H_2O)\}_2(phz)]^{2+}$ cation in $[\{Ru_2(O_2CC(CH_3)_3)_4(H_2O)\}_2(phz)](BF_4)_2$. Hydrogen atoms are omitted for clarity.

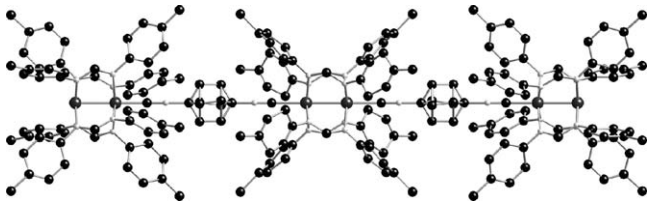

Fig. 5. A hexanuclear complex with "trimer-of-dimers" type [{Rh_2(form)$_4$}$_3$(1,4-dib)$_2$]. Hydrogen atoms are omitted for clarity.

A weak interaction through phenazine was described by comparing the magnetic data of [$Ru_2(O_2CC_2H_5)_4$(phz)]BF_4 [26] and [{Ru_2(chp)$_4$}$_2$(pyz)]$(BF_4)_2$ (chp = 6-chloro-2-hydroxypyridinato) [54]. The tetranuclear species of the "dimer-of-dimers" type can be made depending on the combination of the linking ligand and the dinuclear species. In this context, a hexanuclear complex with "trimer-of-dimers" type has also been prepared for [{Rh_2(form)$_4$}$_3$(1,4-dib)$_2$], which was isolated in the combination of [Rh_2(form)$_4$] (form$^-$ = *N*,*N*′-di-*p*-tolylformamidinate anion) and 1,4-diisocyanobenzene (1,4-dib) (Fig. 5) [55]. A reaction of [$Ru_2(O_2CC(CH_3)_3)_4(H_2O)_2$]$BF_4$ with 2 equiv. of tetramethylpyrazine afforded a polynuclear chain complex [$Ru_2(O_2CC(CH_3)_3)_4(H_2O)_2$(tmpyz)]$_n$ $(BF_4)_n$·$n$$CH_2Cl_2$ (Fig. 6). The crystal structure shows that the $Ru_2(O_2CC(CH_3)_3)_4(H_2O)_2$ units are connected by the hydrogen bonds with the tmpyz molecules, giving an infinite zig-zag chain. The tmpyz molecule does not seem to have an ability to bind to the ruthenium atom because of the steric hindrance of the two methyl groups around the nitrogen atom.

When trifluoroacetic acid is used as the carboxylato group to form a dinuclear ruthenium system, the $Ru_2^{II,II}$ state can be

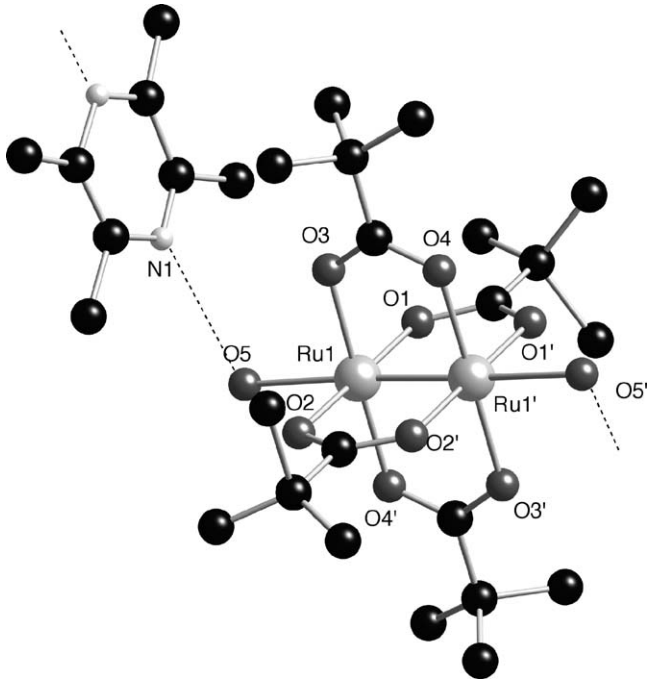

Fig. 6. Crystal structure of [$Ru_2(O_2CC(CH_3)_3)_4(H_2O)_2$(tmpyz)]$^+$ cation moiety in [$Ru_2(O_2CC(CH_3)_3)_4(H_2O)_2$(tmpyz)]$_n(BF_4)_n$. Hydrogen atoms are omitted for clarity.

feasible because of the electron-withdrawing nature of the trifluoromethyl groups. Dunbar and co-workers successfully isolated a one-dimensional chain compound [$Ru_2(O_2CCF_3)_4$(phz)]$_n$ and examined its magnetic property [52], although a solution study on this extended $Ru_2^{II,II}$ chain system had already been reported for [$Ru_2(O_2C(CH_2)_6CH_3)_4$(pyz)] by Wesemann and Chisholm [56]. They found an antiferromagnetic interaction through the phz-bridges with a value of $zJ = -3.0\,cm^{-1}$ between the $Ru_2^{II,II}$ units with $g = 2.0$ and $D = 277\,cm^{-1}$. The zJ value is a little larger in the absolute value compared with those of the phz-bridged adducts of $Ru_2^{II,III}$ unit. The zJ value seems to get smaller in the absolute value when a smaller g value (<2.0) is assumed in the simulation. We prepared the acetate analogues [$Ru_2(O_2CCH_3)_4$(L)]$_n$ (L = pyz, 4,4′-bpy, and dabco), and found that the magnetic data can be explained using the zero-field splitting parameter and neglecting an antiferromagnetic interaction between the $Ru_2^{II,II}$ units (e.g. $g = 2.19$, $D = 290\,cm^{-1}$, for [$Ru_2(O_2CCH_3)_4$(pyz)]$_n$, Table 1) [51]. If we take the antiferromagnetic interaction into account, the g value becomes larger to fit the data ($g = 2.21$, $D = 290$, $zJ = -3\,cm^{-1}$ for [$Ru_2(O_2CCH_3)_4$(pyz)]$_n$, Table 1). Zero-field splitting makes the magnetic moment equal to zero at $T = 0$ K in the case of $Ru_2^{II,II}$ compounds. Therefore, it is usually difficult to evaluate the small J value from the fitting of the magnetic susceptibility data for the $Ru_2^{II,II}$ complexes, because the decrease of the magnetic moment coming from the antiferromagnetic interaction is hidden by the decrease due to the large zero-field splitting, when the temperature is lowered.

Diffuse reflectance spectra of [$Ru_2(O_2CC(CH_3)_3)_4$(L)]$_n$ $(BF_4)_n$ (L = pyz, 4,4′-bpy, and dabco) show a comparatively distinctive band at 422–450 nm with a shoulder at 567–681 nm and a broad band at 1006–1051 nm, which correspond with a distinctive band at 427 nm, a shoulder at 545 nm and a band at 990 nm in [$Ru_2(O_2CC(CH_3)_3)_4(H_2O)_2$]$BF_4$ [31]. These bands can be assigned to the transitions π(Ru–O, Ru_2) → π^*(Ru_2), δ^*/π^*(Ru_2) → σ^*(Ru–O), and δ(Ru_2) → δ^*(Ru_2), respectively [57,58]. It was found in this system that both of the latter two bands show slight red shifts upon coordination of the *N*,*N*′-bidentate ligands. On the other hand, the diffuse reflectance spectra of [$Ru_2(O_2CCH_3)_4$(L)]$_n$ are more featureless, showing a broad peak 500–600 nm in the cases of the pyz and 4,4′-bpy compounds [51]. Further investigation of the spectral properties is needed and is proceeding in our laboratories.

2.2. Redox active ligands

In order to obtain more interesting magnetic properties for one-dimensional assembled complexes of ruthenium carboxylates, a promising direction is the introduction of redox-active organic ligands which are capable of forming an unpaired electron within each linking ligand (Scheme 4). Electrochemical data for some dinuclear metal carboxylates and some redox-active linking ligands are listed in Tables 2 and 3, respectively. *p*-Quinones are good candidates for such linking ligands. We can expect that these linking ligands become paramagnetic *p*-semiquinones once redox reaction occurs with metal carboxylates. Wesemann and Chisholm reported that *p*-benzoquinone

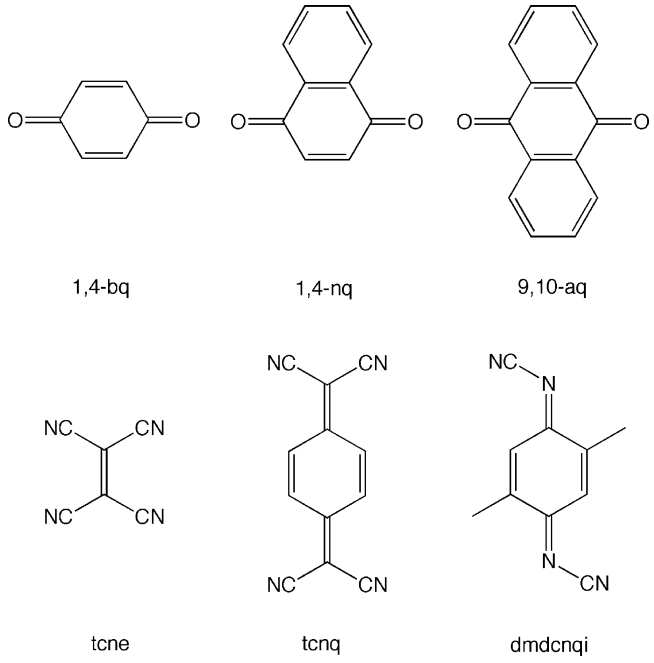

Scheme 4. Structural formulae of *p*-quinone and organic-cyano ligands.

Table 2
Redox potentials for first oxidation of dinuclear metal carboxylates

	$E_{1/2}$ vs. SCE (V) [solvent]	Reference
$[Mo_2(O_2CC_3H_7)_4]$	0.39 [CH_3CN]	[59]
$[Rh_2(O_2CCH_3)_4]$	1.17 [CH_3CN]	[60]
$[Ru_2(O_2CH)_4]$	0.25 [CH_3CN]	[8]
$[Ru_2(O_2CCH_3)_4]$	0.00 [CH_3CN]	[8]
$[Ru_2(O_2CC_2H_5)_4]$	−0.02 [CH_3CN]	[8]
$[Ru_2(O_2CC_3H_7)_4]$	0.00 [CH_2Cl_2]	[61]
$[Ru_2(O_2CC_6H_5)_4]$	0.13 [CH_3CN]	[8]
$[Ru_2(O_2CCF_3)_4]$	1.17 [CH_2Cl_2]	[9]

undergoes a redox reaction with $[Ru_2(O_2C(CH_2)_6CH_3)_4]$ and the $[Ru_2(O_2C(CH_2)_6CH_3)_4]^+$[semiquinone]$^{-\bullet}$ species can be isolated [56].

We performed reactions of 1,4-benzoquinone (1,4-bq), 1,4-naphthoquinone (1,4-nq), and 9,10-anthraquinone (9,10-aq) with ruthenium(II, III) pivalate under argon [42,44]. However, the isolated compounds $[Ru_2(O_2CC(CH_3)_3)_4L]_n(PF_6)_n$ (L = 1,4-bq, 1,4-nq), were air-sensitive and far from sustainable for magnetic susceptibility measurements. In the case of 9,10-aq, we could isolate a tetranuclear compound of $[\{Ru_2(O_2CC(CH_3)_3)_4(H_2O)\}_2(9,10\text{-aq})](BF_4)_2$ and a small amount of polynuclear chain compound $[Ru_2(O_2CC(CH_3)_3)_4(9,10\text{-aq})]_n$; crystal structures are shown (Figs. 7 and 8). The magnetic susceptibility data of $[\{Ru_2(O_2CC(CH_3)_3)_4(H_2O)\}_2(9,10\text{-aq})](BF_4)_2$ shows that the magnetic interaction between the two ruthenium cores through the bridging 9,10-aq is negligibly small [42]. Jimenez-Aparicio et al. observed reduction of ruthenium(II, III) carboxylates with hydroquinone in the presence of piperidine or triethylamine [64]. They applied this reaction to prepare ruthenium(II, II) carboxylates $[Ru_2(O_2CR)_4(CH_3OH)_2]$ (R = CH_3, C_6H_5, $C(C_6H_5)_2CH_3$, C_6H_4-*p*-OCH_3, C_6H_4-*p*-$C(CH_3)_3$). An interesting one-pot reaction of ruthenium(II, III) acetate with arylcarboxylic acids in *N*,*N*-dimethylaniline giving ruthenium(II, II) arylcarboxylates, was reported [65]. In this case, *N*,*N*-dimethylaniline seems to reduce the $Ru_2^{II,III}$ cores.

In the field of compounds with organic electron acceptors, organic cyano molecules such as tetracyanoethylene (tcne) afford a rich research area (Scheme 4) [66–68]. The organic acceptors have positive redox potentials (versus SCE) (Table 3) and we can expect redox reactions with dinuclear metal carboxylates to form ferrimagnetic chain compounds as shown in Scheme 5. From an early stage, Dunbar noticed the importance of these organic acceptors and tried to incorporate them with metal–metal bond clusters into solid-state materials [69], although the original study describing a treatment of a solution of the quadruply-bonded Mo_2(tmtaa)$_2$ (tmtaa = dibenzotetramethyltetraaza[14]annulene) with tcne was reported by Giraudon et al. [70]. The tetranuclear complex of "dimer-of-dimers" $[\{Re_2Cl_4(dppm)_2\}_2(tcnq)]$ (dppm = 1,2-bis(diphenylphosphanyl)methane, tcnq = 7,7,8,8-tetracyanoquinodimethane), where the tcnq molecule bridges the two Re dimers, is the first example of an electron-transferred complex of tcnq with a metal–metal bond donor [71]. Reactions of $Ru_2(O_2CR)_4Cl$ (R = C_2H_5, C_3H_7, $C(CH_3)_3$) with Li(tcne) gave a black powder of $Ru_2(O_2CR)_4$(tcne) [72]. Interestingly, the magnetic moment of $Ru_2(O_2CC(CH_3)_3)_4$(tcne) behaves like a ferrimagnet with a Neel temperature of 100 K. Blue/black to purple products of $Ru_2(O_2CR)_4$(dmdcnqi) (R = H,

Table 3
Redox potentials for first reduction of redox-active ligands

	$E_{1/2}$ vs. SCE (V) [solvent]	Reference
tcne	0.23 [CH_3CN]	[62]
tcnq	0.19 [CH_3CN]	[62]
2,5-dmdcnqi	0.06 [CH_3CN]	[62]
$[C(CN)_3]^-$	1.28 [CH_3CN]	[62]
ddq	0.51 [CH_3CN]	[63]
1,4-bq	−0.51 [CH_3CN]	[63]
1,4-nq	−0.71 [CH_3CN]	[63]
9,10-aq	−0.94 [CH_3CN]	[63]

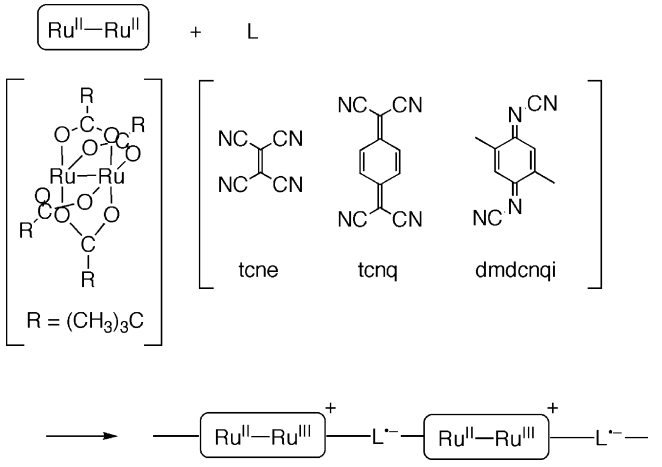

Scheme 5. Reactions of ruthenium(II, II) pivalate with organic-cyano electron acceptors.

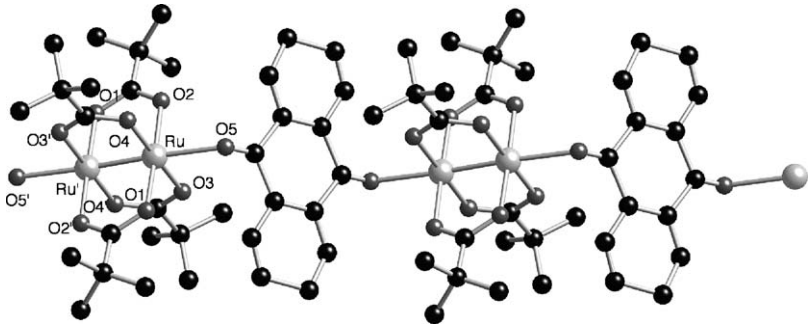

Fig. 7. Crystal structure of $[Ru_2(O_2CC(CH_3)_3)_4(9,10\text{-aq})]_n$. Hydrogen atoms are omitted for clarity.

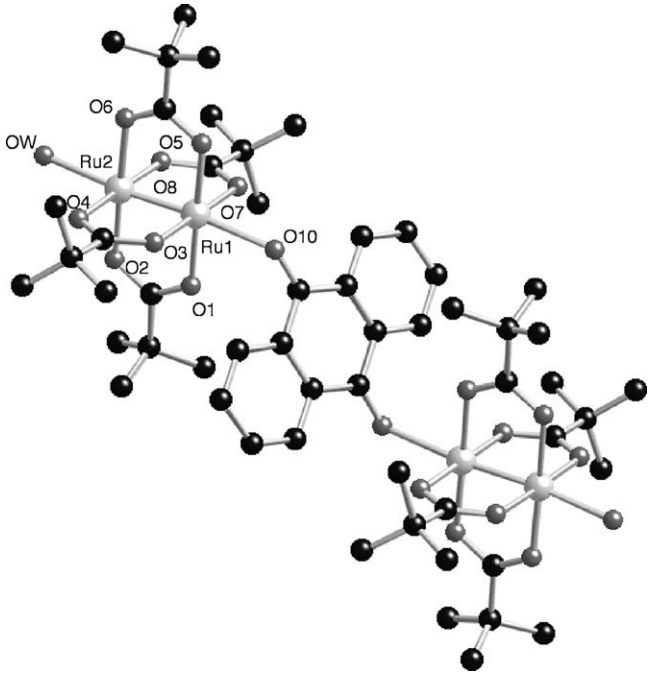

Fig. 8. Crystal structure of $[\{Ru_2(O_2CC(CH_3)_3)_4(H_2O)\}_2(9,10\text{-aq})](BF_4)_2$. Hydrogen atoms are omitted for clarity.

CH_3, C_2H_5, C_6H_5, C_6H_4-*p*-CH_3; dmdcnqi = 2,5-dimethyl-*N*,*N*′-dicyanobenzoquinonediimine) were prepared in THF under a dry inert atmosphere from either reaction of $Ru_2(O_2CR)_4$ and dmdcnqi or $Ru_2(O_2CR)Cl$ and Na[dmdcnqi]$_2$ [73,74]. In the diffuse reflectance spectra, the band corresponding to $\pi(Ru\text{–}O,\ Ru_2) \rightarrow \pi^*(Ru_2)$ absorption at 425 nm for $Ru_2(O_2CR)_4^+$ was obscured by the strong broad 580 nm feature in these compounds. The magnetic properties of $Ru_2(O_2CR)_4$(dmdcnqi) (R = CH_3, C_6H_4-*p*-CH_3) are antiferromagnetic with Neel temperatures of 27 and 46 K, respectively. Wesemann and Chisholm observed that tcne undergoes an oxidation of $[Ru_2(O_2C(CH_2)_6CH_3)_4]$ and induces structural rearrangement of the Ru_2 core in toluene [56].

We obtained chain complexes by reactions of ruthenium(II, II) pivalate dimer with tcne, tcnq, and dmdcnqi [75]. The variation of magnetic moment with temperature of $[Ru_2(O_2CC(CH_3)_3)_4L]_n$ (L = tcne and dmdcnqi) shows ferrimagnetic behavior in an alternating one-dimensional arrangement of 3/2 and 1/2 spins. A similar result was found in Dunbar's compound obtained from a reaction of $Ru_2(O_2CR)_4Cl$ and Li(tcne) [72]. On the other hand, the magnetic moment of $[Ru_2(O_2CC(CH_3)_3)_4(tcnq)]_n$ decreases steadily with decrease of temperature. This behavior may be due to the existence of magnetically isolated $Ru_2^{II,III}$-tcnq$^{-\bullet}$ units in which the antiferromagnetic interaction operates between the Ru(II, III) dimer and the radical anion. A chain compound $[Ru_2(O_2CC(CH_3)_3)_4(dmdcnqi)]_n(BF_4)_n$, was also prepared by a reaction of ruthenium(II, III) pivalate dimer with dmdcnqi in benzene [44]. In this case, the bridging dmdcnqi is neutral and has no spin. The magnetic interaction between the $Ru_2^{II,III}$ cores is very weak through the linkage ligand ($zJ = -0.30\ cm^{-1}$). An interesting tetranuclear species $[\{Ru_2(O_2CC(CH_3)_3)_4(H_2O)\}_2(tcnq)](BF_4)_2$ was isolated from a reaction of ruthenium(II, III) pivalate with tcnq [43]. The X-ray structure analysis revealed a "dimer-of-dimers" structure where

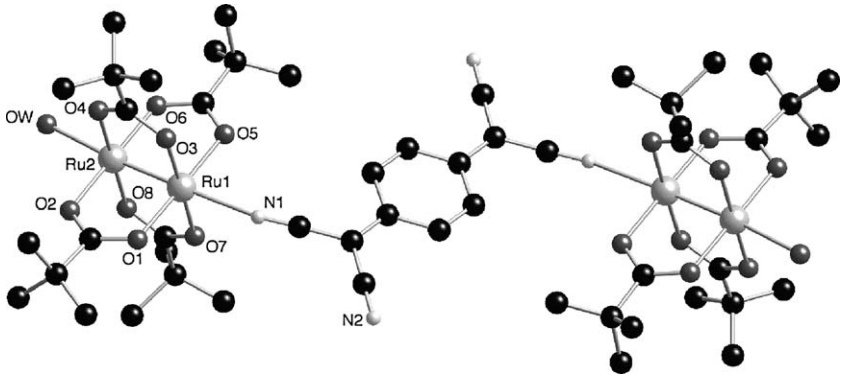

Fig. 9. Crystal structure of $[\{Ru_2(O_2CC(CH_3)_3)_4(H_2O)\}_2(tcnq)](BF_4)_2$. Hydrogen atoms are omitted for clarity.

the neutral tcnq molecule bridges the two $Ru_2^{II,III}$ units in a *trans* fashion (Fig. 9). In this compound, a weak antiferromagnetic interaction through the tcnq bridge between the two dinuclear units ($zJ = -0.30\,cm^{-1}$) was observed.

Dunbar and co-workers treated dicyanamide ($N(CN)_2^-$) and tricyanomethanide ($C(CN)_3^-$) ions to ruthenium(II, III) acetate and obtained chain compounds $[Ru_2(O_2CCH_3)_4(L)]$ (L = $N(CN)_2^-$ and $C(CN)_3^-$) [45]. The crystal structures show the alternating zig-zag arrangement of the $Ru_2^{II,III}$ units and L anions. The fitting parameters of the magnetic data with Eq. (1) are $g = 2.16$, $D = 63.3$, $zJ = -0.33\,cm^{-1}$ and $g = 2.15$, $D = 58.0$, $zJ = -0.22\,cm^{-1}$, respectively.

2.3. Organic radical ligands

A most promising way to obtain ferrimagnetic type compounds is the introduction of organic radical molecules such as nitroxide having bridging ability instead of the diamagnetic bridging groups (Scheme 6). The first isolation of nitroxide radical adducts of dinuclear carboxylates with metal–metal bonds was performed for rhodium carboxylates

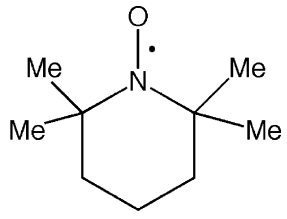

tempo

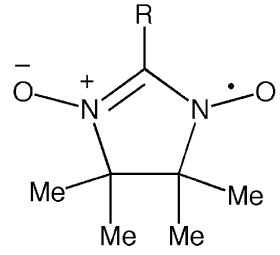

R = -CH_3 nitme

-C_2H_5 nitet

 nitph

m-nitpy

p-nitpy

Scheme 6. Structural formulae of nitroxide ligands.

by Cotton and Felthouse [76] and the crystal structures of $[Rh_2(O_2CCF_3)_4(tempol)_2]$ (tempol = 4-hydroxy-2,2,6,6- tetramethylpiperidine-1-oxyl) and $[Rh_2(O_2CCF_3)_4(H_2O)_2(dtbn)_2]$ (dtbn = di-*tert*-butyl nitroxide) were reported. The axial ligands for $Rh_2(O_2CCF_3)_4$ core are oxygen donors but not from the nitroxyl groups as originally intended. The tempol ligands coordinate to the Rh atoms in the former compound through their hydroxyl oxygen atoms at a distance of 2.240(3) Å. In the latter case, the nitroxide oxygen atoms are hydrogen bonded to the axial water molecules. Later, analogous bis(nitroxide) adducts $[Rh_2(O_2CR)_4(tempo)_2]$ (R = CF_3, C_3F_7, and C_6F_5) were prepared [77,78]. In these complexes, the two tempo oxygen atoms occupy the axial positions of the $Rh_2(O_2CR)_4$ core. Hendrickson et al. observed a strong antiferromagnetic interaction of the two axial nitroxide spins through the metal–metal bond in these compounds ($J = -239$, -269, and $-184\,cm^{-1}$, respectively) and attributed this interaction to $Rh_2\pi^*$–$NO\pi^*$ back bonding. A further analogous bis(nitroxide) adduct $[Rh_2(O_2CCF_3)_4(nitph)_2]$, was prepared by Rey et al. using 2-phenyl-4,4,5,5-tetramethyl-4,5-dihydro-1*H*-imidazolyl-1-oxyl 3-*N*-oxide (nitph) [79,80]. They isolated a chain compound $[Rh_2(O_2CCF_3)_4(nitme)]_n$ by using a nitronyl nitroxide with less bulky substituent group at the two-position, 2,4,4,5,5-pentamethyl-4,5-dihydro-1*H*-imidazol-1-oxyl 3-*N*-oxide (nitme). These complexes exhibited fairly large antiferromagnetic interactions ($2J = -167.2$ and $-197.6\,cm^{-1}$) through the metal–metal bonds. Further, they isolated a bis(nitroxide) adduct and chain compound also by using an imino nitroxide, 2,4,4,5,5-pentamethyl-4,5-dihydro-1*H*-imidazol-1-oxyl (imme). Rey and co-workers ascribed the antiferromagnetic coupling to the σ mechanism due to the interaction between the nitroxide radicals through the Rh_2 σ orbital in place of the π mechanism by Hendrickson.

With respect to ruthenium carboxylates, Rey and coworkers tried to isolate chain compounds, however, they obtained bis(tempo) adducts of ruthenium(II, II) carboxylate $[Ru_2(O_2CCF_3)_4(tempo)_2]$ and $[Ru_2(O_2CC_6F_5)_4(tempo)_2]$ [81]. These compounds afford an interesting magnetic system consisting of exchange interactions of the radical ($S = 1/2$) spins through the Ru–Ru bond and the diruthenium(II, II) core ($S = 1$)—radical ($S = 1/2$) spins as well as a large zero-field splitting within the dinuclear core. The analysis showed that the magnetic interaction between the free radical and the dinuclear metal spins is predominant ($J = -263$ and $-234\,cm^{-1}$). They attributed the interaction to the overlapping of the π^* orbitals of Ru–Ru bonds with the π^* orbital of the NO groups.

We examined ruthenium(II, III) systems using a variety of nitroxides [34,82–91]. Ruthenium pivalate which was not considered to be advantageous for enforcing coordination of weak donor groups such as nitroxides, was selected as a metal source because of the higher solubility in organic solvents. Reaction of $[Ru_2(O_2CC(CH_3)_3)_4(H_2O)_2]BF_4$ with tempo in dichloromethane did not give any tempo adduct but the starting material was recovered as reddish-brown crystals of $[Ru_2(O_2CC(CH_3)_3)_4(H_2O)_2]BF_4{\cdot}CH_2Cl_2$ [32]. The axial sites of the dinuclear $Ru_2^{II,III}$ core are occupied by the oxygen atoms of water molecules. In the crystal, the dinuclear cations are hydrogen-bonded to the tetrafluorob-

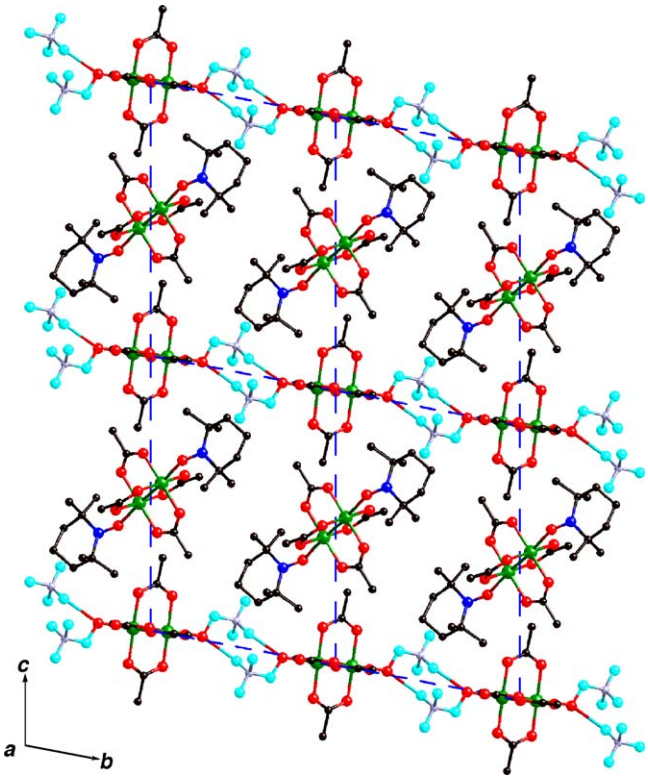

Fig. 10. Crystal packing of $[Ru_2(O_2CC(CH_3)_3)_4(tempo)_2]$ $[Ru_2(O_2CC(CH_3)_3)_4(H_2O)_2](BF_4)_2$. Hydrogen atoms are omitted for clarity.

orate ions through axial water molecules to form a two-dimensional sheet. When the reaction was performed in benzene, a mixed cation complex $[Ru_2(O_2CC(CH_3)_3)_4(tempo)_2]$ $[Ru_2(O_2CC(CH_3)_3)_4(H_2O)_2](BF_4)_2$, was isolated [82]. The crystal structure shows that the bis(nitroxide)-adducts cations are incorporated into the space between the chains made up of $[Ru_2(O_2CC(CH_3)_3)_4(H_2O)_2]^+$ and BF_4^-, where each ruthenium pivalate cation is connected with two tetrafluoroborate ions by hydrogen bonds (Fig. 10). These reactions were performed at room temperature. When we refluxed the benzene solution

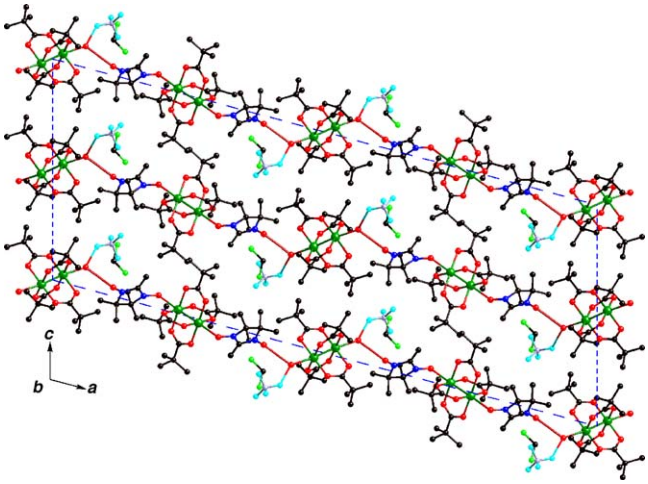

Fig. 11. Crystal packing of $[\{Ru_2(O_2CC(CH_3)_3)_4(nitme)_2\}\{Ru_2(O_2CC(CH_3)_3)_4(H_2O)_2\}](BF_4)_2$. Hydrogen atoms are omitted for clarity.

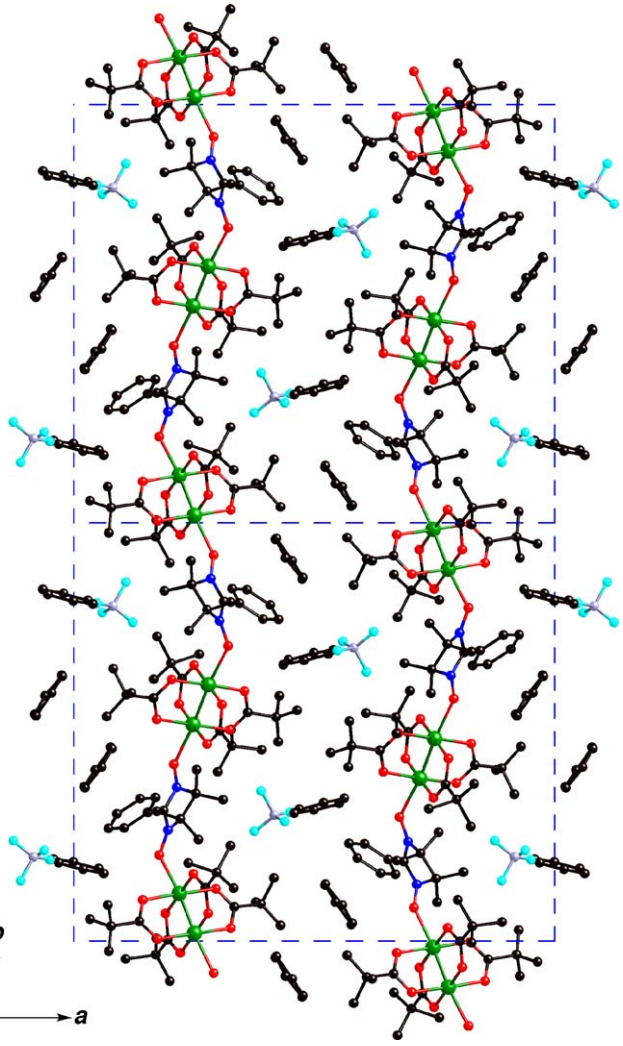

Fig. 12. Crystal packing of $[Ru_2(O_2CC(CH_3)_3)_4(nitph)]_n(BF_4)_n$. Hydrogen atoms are omitted for clarity.

of ruthenium pivalate and tempo, we obtained the bis(tempo) adduct $[Ru_2(O_2CC(CH_3)_3)_4(tempo)_2]BF_4$ [34]. Recrystallization of this adduct from benzene afforded the hydrated species $[Ru_2(O_2CC(CH_3)_3)_4(H_2O)_2]BF_4$. These observations mean that coordination ability of tempo to ruthenium is relatively weak and water molecules tend to occupy the axial sites of the dinuclear core.

The magnetic moment of $[Ru_2(O_2CC(CH_3)_3)_4(H_2O)_2]BF_4$ is $4.31\mu_B$ at 300 K and gradually decreases to $3.24\mu_B$ at 2.5 K. The variation with temperature could be explained by introduction of the zero-field splitting parameter $D = 60\,cm^{-1}$ and $g_{Ru} = 2.15$ [34]. The magnetic data of $[Ru_2(O_2CC(CH_3)_3)_4(tempo)_2]BF_4$ were analyzed by the van Vleck equation based on the Heisenberg model of 1/2–3/2–1/2 spin system (Scheme 7), giving J_{M-R} (for $Ru_2^{II,III}$—radical interaction) $= -80\,cm^{-1}$, J_{R-R} (for radical–radical interaction through Ru–Ru bond) $= 0$, $D = 0\,cm^{-1}$, $g_{Ru} = 2.08$, $g_{nitroxide} = 2.00$ (fixed) [34]. With respect to $[Ru_2(O_2CC(CH_3)_3)_4(tempo)_2]$ $[Ru_2(O_2CC(CH_3)_3)_4(H_2O)_2](BF_4)_2$, $J_{M-R} = -130$, $J_{R-R} = 0$, $D = 0\,cm^{-1}$, $g_{Ru} = 2.117$, $g_{nitroxide} = 2.00$ (fixed) were estimated for the bis(tempo) adduct moiety [82].

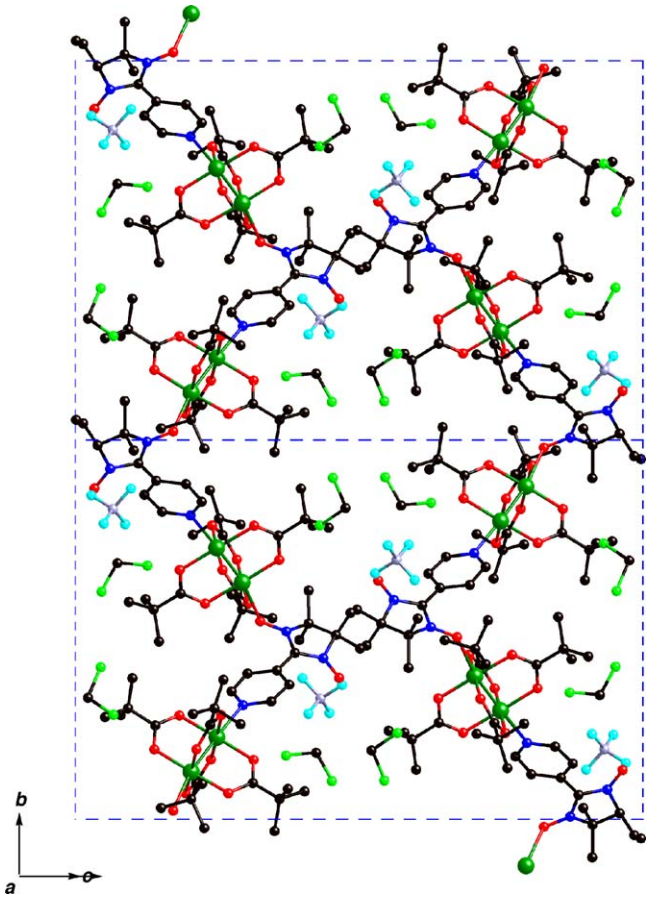

Fig. 13. Crystal packing of $[Ru_2(O_2CC(CH_3)_3)_4(p\text{-nitpy})]_n(BF_4)_n$. Hydrogen atoms are omitted for clarity.

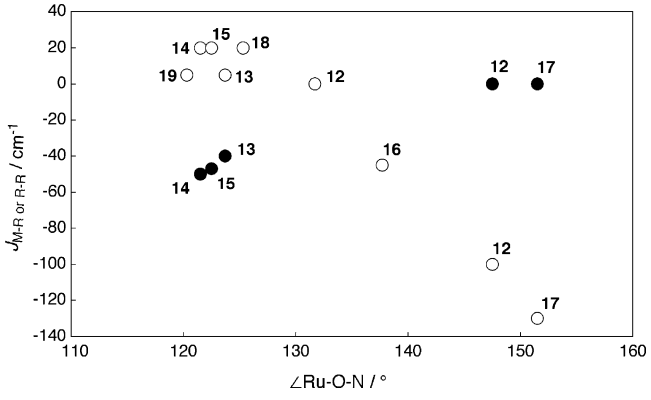

Fig. 14. Plots of the experimental $J_{M–R}$ (◯) and $J_{R–R}$ (●) values vs. Ru–O_{ax}–N bond angles. Numbers refer to the complexes listed in Table 4.

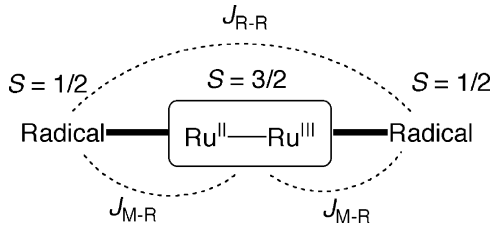

Scheme 7. The 1/2–3/2–1/2 spin system in bis(radical) adducts.

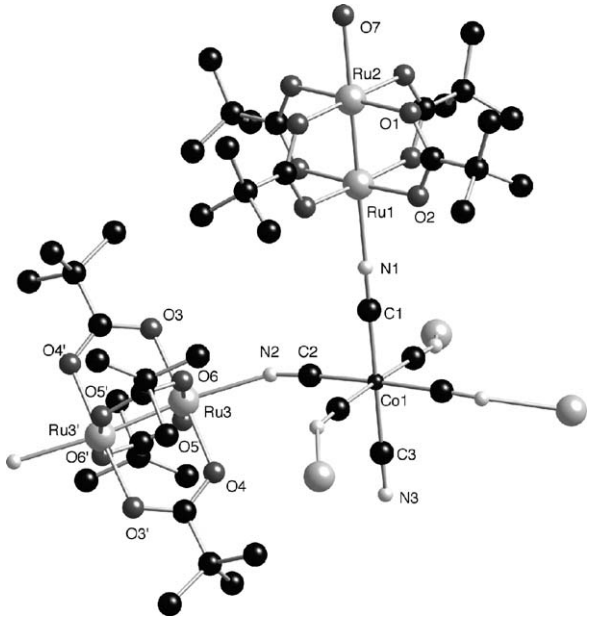

Fig. 15. Asymmetric unit of the crystal structure of $[\{Ru_2(O_2CC(CH_3)_3)_4\}_3(H_2O)Co(CN)_6]_n{\cdot}4nH_2O$. Hydrogen atoms are omitted for clarity.

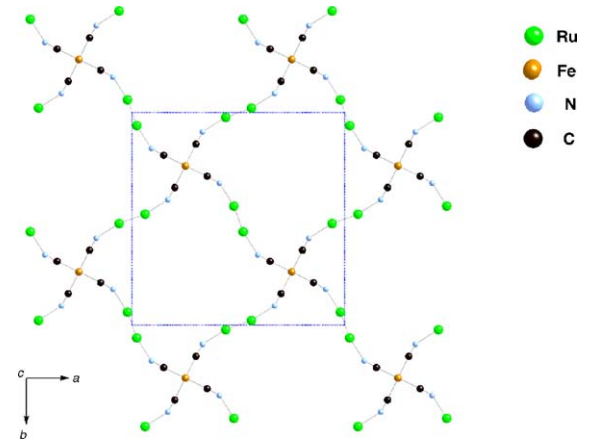

Fig. 16. 2D network of $[\{Ru_2(O_2CC(CH_3)_3)_4\}_3(H_2O)Fe(CN)_6]_n{\cdot}4nH_2O$ onto the *ab* plane. Hydrogen atoms are omitted for clarity.

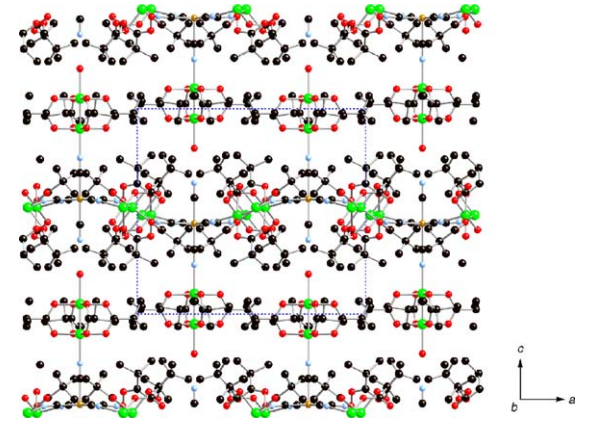

Fig. 17. 3D network of $[\{Ru_2(O_2CC(CH_3)_3)_4\}_3(H_2O)Fe(CN)_6]_n{\cdot}4nH_2O$. Hydrogen atoms are omitted for clarity.

When we employed 2,4,4,5,5-pentamethyl-4,5-dihydro-1*H*-imidazol-1-oxyl 3-*N*-oxide (nitme) and 2-ethyl-4,4,5,5-tetramethyl-4,5-dihydro-1*H*-imidazol-1-oxyl 3-*N*-oxide (nitet) as the radical ligands, chain complexes $[\{Ru_2(O_2CC(CH_3)_3)_4L_2\}\{Ru_2(O_2CC(CH_3)_3)_4(H_2O)_2\}](BF_4)_2$ (L = nitme, nitet), were isolated in addition to bis(nitroxide) adducts $[Ru_2(O_2CC(CH_3)_3)_4L_2]BF_4$ (L = nitme, nitet), depending on the $Ru_2^{II,III}$:radical molar ratio employed for the reaction [86,89]. In the bis(nitroxide) adducts, each axial site of the Ru_2 core is occupied by an oxygen atom of the N–O group of the nitroxide. One of the two N–O groups of the nitroxide molecule does not participate in coordination, resulting in the slightly shorter N–O length. Like the tempo case, there are two kinds of dinuclear Ru(II, III) units in the crystals of the chain complexes. However, the arrangement of the dinuclear units are different from that of $[Ru_2(O_2CC(CH_3)_3)_4(tempo)_2][Ru_2(O_2CC(CH_3)_3)_4(H_2O)_2](BF_4)_2$. The dinuclear units are connected by using hydrogen bonds between the uncoordinated N–O groups of the nitroxides and the coordinated water molecules of the neighboring dimer units, forming a zig-zag chain structure with an alternated arrangement of the bis(nitroxide)-Ru_2 and dihydrate-Ru_2 units (Fig. 11). In the case of the tempo adduct, the bis(tempo)-Ru_2 units do not form any hydrogen bonds with the dihydrate-Ru_2 units, because tempo has only one N–O group within the molecule. The magnetic properties of bis(nitroxide) adducts $[Ru_2(O_2CC(CH_3)_3)_4L_2]BF_4$ (L = nitme, nitet), could be interpreted with the van Vleck equation based on the Heisenberg model of 1/2–3/2–1/2 spin system. The best fit was obtained with $J_{M-R} = 5$, $J_{R-R} = -40$, $D = 20\,cm^{-1}$, $g_{Ru} = 2.40$, $g_{nitroxide} = 2.00$ (fixed) and $J_{M-R} = 5$, $J_{R-R} = -40$, $D = 40\,cm^{-1}$, $g_{Ru} = 2.25$, $g_{nitroxide} = 2.00$ (fixed), respectively. In the cases of the chain compounds $[\{Ru_2(O_2CC(CH_3)_3)_4L_2\}\{Ru_2(O_2CC(CH_3)_3)_4(H_2O)_2\}](BF_4)_2$ (L = nitme, nitet), we set the zero-field splitting for the dihydrated Ru_2 dimer at $D' = 60\,cm^{-1}$. The magnetic parameters obtained are listed in Table 4. The positive J_{M-R} value ($20\,cm^{-1}$) and negative J_{R-R} (-50 and $-47\,cm^{-1}$) values were found for these hydrogen-bonded chain compounds.

Adopting a nitronyl nitroxide with a more hydrophobic group, 2-phenyl-4,4,5,5-tetramethyl-4,5-dihydro-1*H*-imidazolyl-1-oxyl 3-*N*-oxide (nitph), we met different situations. When the reaction of ruthenium pivalate with nitph was carried out in dichloromethane, an unsymmetric adduct $[Ru_2(O_2CC(CH_3)_3)_4(nitph)(H_2O)]BF_4$, was isolated [88]. The crystal structure shows that one N–O group of nitph coordinates to the Ru_2 core at one of its two axial sites and the other is occupied by a water molecule. The axial water molecule is further hydrogen-bonded to the tetrafluoroborate ions to form a hydrogen-bonded tetranuclear species. The magnetic data could be explained by the spin pair model with $J_{M-R} = -45\,cm^{-1}$, $g_{Ru} = 2.34$, $g_{nitroxide} = 2.00$, $D = -30\,cm^{-1}$, considering spin-coupling between the Ru_2 core ($S = 3/2$) and nitph ($S = 1/2$) spins. When the reaction was performed in benzene, a chain compound $[Ru_2(O_2CC(CH_3)_3)_4(nitph)]_n(BF_4)_n$ which we had intended initially, was obtained [83,84]. The crystal structure shows a zig-zag chain structure with an alternating arrangement of the $Ru_2^{II,III}$ dimer and nitph (Fig. 12). We expected that this compound would show ferrimagnetic behavior, because the chain has an alternating arrangement of 3/2 ($Ru_2^{II,III}$ core) and 1/2 (nitph) spins. However, the magnetic behavior is not

Table 4
Structural parameters and *J* values for the axially O-bonded nitroxide complexes of $[M_2(O_2CR)_4]^{0/+}$ (M = Ru and Rh)

Complex	M–O_{ax} (Å)	M–O_{ax}–N (°)	J_{M-R} (cm^{-1})	J_{R-R} (cm^{-1})	Reference
$[Ru_2(O_2CC(CH_3)_3)_4(nitph)]_n(BF_4)_n$ (**12**)	2.264(8), 2.236(8)	131.7(7), 147.5(7)	0, −100	–[a]	[84]
$[Ru_2(O_2CC(CH_3)_3)_4(nitme)_2]BF_4 \cdot 2CH_2Cl_2$ (**13**)	2.239(4)	123.7(4)	5	−40	[89]
$[\{Ru_2(O_2CC(CH_3)_3)\}_4(nitme)_2]\{Ru_2(O_2CC(CH_3)_3)_4(H_2O)_2\}]_n(BF_4)_{2n} \cdot 2nCH_2Cl_2$ (**14**)	2.269(8)	121.5(6)	20	−50	[89]
$[\{Ru_2(O_2CC(CH_3)_3)\}_4(nitet)_2]\{Ru_2(O_2CC(CH_3)_3)\}_4(H_2O)_2\}]_n(BF_4)_{2n} \cdot 2nCH_2Cl_2$ (**15**)	2.270(9)	122.5(7)	20	−47	[89]
$[Ru_2(O_2CC(CH_3)_3)_4(nitph)(H_2O)]BF_4$ (**16**)	2.260(6)	137.7(5)	−45		[88]
$[Ru_2(O_2CC(CH_3)_3)_4(tempo)_2][Ru_2(O_2CC(CH_3)_3)_4(H_2O)_2](BF_4)_2$ (**17**)	2.184(3)	151.5(3)	−130	0	[82]
$[Ru_2(O_2CC(CH_3)_3)_4(p\text{-nitpy})]_n(BF_4)_n$ (**18**)	2.286(7)	125.3(6)	20	–[b]	[90]
$[Ru_2(O_2CC_2H_5)_4(m\text{-nitpy})]_n(BF_4)_n$ (**19**)	2.295(4)	120.0(3)	5	–[b]	[91]
$[Ru_2(O_2CCF_3)_4(tempo)_2]$	2.136(5)	158.2(3)	−263	0	[81]
$[Rh_2(O_2CCF_3)_4(tempo)_2]$	2.220(2)	138.0(1)	–[b]	−239	[78]
$[Rh_2(O_2CC_3F_7)_4(tempo)_2]$	2.235(5)	134.2(4)	–[c]	−269	[78]
$[Rh_2(O_2CCF_3)_4(nitph)_2]$	2.239(3)	122.7(3)	–[c]	−83.6	[80]
$[Rh_2(O_2CCF_3)_4(nitme)]_n$	2.268(5), 2.254(5)	118.3(4), 121.3(4)	–[c]	−98.8	[80]

[a] The Ru–O–N axial bond angle 131.7(7)° may be suitable for interaction between the radicals through the Ru–Ru bond via the σ-pathway mechanism (see text). However, the axial angle 147.5(7)° at the other axial side of the dinuclear core is unfavorable for interaction, causing no observation of interaction between the radicals [84].

[b] One of the two axial sites of dinuclear Ru(II, III) core is only coordinated by the N–O group of the radical [88,90].

[c] The dinuclear Rh(II, II) core is diamagnetic.

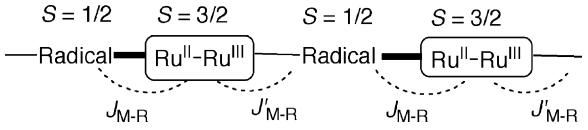

Scheme 8. The 1/2–3/2 spin system in chain compounds.

ferrimagnetic. The data can be interpreted with the spin pair model ($J'_{M-R} = 0\,cm^{-1}$ in Scheme 8) with $J_{M-R} = -100\,cm^{-1}$, $g_{Ru} = 2.00$, $g_{nitroxide} = 2.00$, and $D = 65\,cm^{-1}$.

We extended our nitroxide ligands to nitronyl nitroxides having a pyridyl group, 2-(4-pyridyl)-4,4,5,5-tetramethyl-4,5-dihydro-1*H*-imidazolyl-1-oxyl 3-*N*-oxide (*p*-nitpy) and 2-(3-pyridyl)-4,4,5,5-tetramethyl-4,5-dihydro-1*H*-imidazolyl-1-oxyl 3-*N*-oxide (*m*-nitpy) hoping to obtain higher dimensionally assembled systems by virtue of the strong coordinating ability of the pyridyl nitrogen [85,87,90,91]. The reactions of ruthenium(II, III) pivalate with these radicals under the conditions using more than two-times as much as the nitroxides to the ruthenium pivalate afforded bis(nitroxide) adducts $[Ru_2(O_2CC(CH_3)_3)_4L_2]X$ (L = *p*-nitpy, *m*-nitpy; $X = BF_4^-$, $B(C_6H_5)_4^-$). The crystal structures of $[Ru_2(O_2CC(CH_3)_3)_4L_2]BF_4$ (L = *p*-nitpy, *m*-nitpy) revealed that the axial positions of the Ru_2 core are occupied by the pyridyl nitrogen atoms of the two nitronyl nitroxides. The magnetic properties of bis(nitroxide) adducts $[Ru_2(O_2CC(CH_3)_3)_4L_2]X$ (*p*-nitpy, *m*-nitpy; $X = BF_4^-$, $B(C_6H_5)_4^-$), could be interpreted with the magnetic parameters, $J_{M-R} = -1.0$, $J_{R-R} = 0\,cm^{-1}$, and $J_{M-R} = 0.8$ or $1.4\,cm^{-1}$, $J_{R-R} = 0\,cm^{-1}$, for *p*-nitpy and *m*-nitpy adducts, respectively. The sign of the J_{M-R} value is different, reflecting the significant difference in the magnetic behavior in these complexes. This difference can be explained by the spin-polarization mechanism [92]. When we employed an equimolar amount of $Ru_2^{II,III}$ salts and the pyridyl nitroxides, the 1:1 chain complexes $[Ru_2(O_2CC(CH_3)_3)_4L]_n(BF_4)_n$ (L = *p*-nitpy, *m*-nitpy) were obtained. The crystal structure of $[Ru_2(O_2CC(CH_3)_3)_4(p\text{-nitpy})]_n(BF_4)_n$ shows the zig-zag chain structure with alternate arrangement of $Ru_2^{II,III}$ dimers and *p*-nitpy radicals (Fig. 13). One of the axial sites of the Ru_2 dimer is occupied by the pyridyl nitrogen of *p*-nitpy with a separation of Ru–N = 2.260(9) Å. The other site is occupied by the one of the two N–O groups of *p*-nitpy with a Ru–O distance of 2.286(7) Å. The magnetic moments at room temperature are similar to each other ($4.75\mu_B$ for $[Ru_2(O_2CC(CH_3)_3)_4(m\text{-nitpy})]_n(BF_4)_n$, $4.89\mu_B$ for $[Ru_2(O_2CC(CH_3)_3)_4(p\text{-nitpy})]_n(BF_4)_n$). However, the low temperature profiles are different: the moment of $[Ru_2(O_2CC(CH_3)_3)_4(m\text{-nitpy})]_n(BF_4)_n$ is nearly constant with decrease of temperature down to 100 K and then falls to the value of $2.83\mu_B$, while the moment of $[Ru_2(O_2CC(CH_3)_3)_4(p\text{-nitpy})]_n(BF_4)_n$ increases to a maximum value of $5.70\mu_B$ at 8 K and then rapidly decreases to reach the value of $3.89\mu_B$ at 2 K. The magnetic data were analyzed by combination of the spin pair model and molecular field approximation ($J'_{M-R} \neq 0\,cm^{-1}$ in Scheme 8). We estimated the magnetic interaction (J_{M-R}) between the $Ru_2^{II,III}$ ($S = 3/2$) and the nitroxide radical ($S = 1/2$) through the N–O group by the spin pair model. The magnetic interaction through the pyridyl group (J'_{M-R}) was estimated by the molecular field approximation. The parameters obtained are $J_{M-R} = 0.3\,cm^{-1}$, $J'_{M-R} = -0.4\,cm^{-1}$, $D = 40\,cm^{-1}$, $g_{Ru} = 2.32$, $g_{nitroxide} = 2.00$ (fixed) and $J_{M-R} = 20$, $J'_{M-R} = -0.45\,cm^{-1}$, $D = 50\,cm^{-1}$, $g_{Ru} = 2.23$, $g_{nitroxide} = 2.00$ (fixed) for $[Ru_2(O_2CC(CH_3)_3)_4(m\text{-nitpy})]_n(BF_4)_n$ and $[Ru_2(O_2CC(CH_3)_3)_4(p\text{-nitpy})]_n(BF_4)_n$, respectively. The ferromagnetic behavior of $[Ru_2(O_2CC(CH_3)_3)_4(p\text{-nitpy})]_n(BF_4)_n$ can be interpreted by taking into consideration that the *p*-nitpy radical ferromagnetically interacts with $Ru_2^{II,III}$ unit through the pyridyl nitrogen ($J'_{M-R} = -0.45\,cm^{-1}$) as well as through the nitroxide oxygen ($J_{M-R} = 20\,cm^{-1}$). In this manner, the antiferromagnetic behavior of $[Ru_2(O_2CC(CH_3)_3)_4(m\text{-nitpy})]_n(BF_4)_n$ may be due to the antiferromagnetic interaction through the pyridyl group ($J'_{M-R} = -0.4\,cm^{-1}$) rather than the ferromagnetic interaction through the N–O group ($J_{M-R} = 0.3\,cm^{-1}$). However, we had no crystal structure for the latter complex because of the difficulty of crystallization. Therefore, we extended our systems to ruthenium propionate in the hope of obtaining good crystals for the *m*-nitpy adduct and isolated bis(nitroxide) adducts $[Ru_2(O_2CC_2H_5)_4L_2]BF_4$ (L = *p*-nitpy, *m*-nitpy), and chain compounds $[Ru_2(O_2CC_2H_5)_4(p\text{-nitpy})]_n(BF_4)_n$ and $[Ru_2(O_2CC_2H_5)_4(m\text{-nitpy})]_n(PF_6)_n$ [91]. The crystal structure of $[Ru_2(O_2CC_2H_5)_4(p\text{-nitpy})_2]BF_4$ shows a similar structure to that of $[Ru_2(O_2CC(CH_3)_3)_4(p\text{-nitpy})_2]BF_4$. The structural effect on the bis-adduct due to the change from *t*-butyl to ethyl group in the dinuclear core could not be found. The bis(*m*-nitpy) adduct has an antiferromagnetic interaction through the pyridyl group ($J_{M-R} = -1.6\,cm^{-1}$), on the other hand, the bis(*p*-nitpy) adduct has a ferromagnetic interaction through the pyridyl group ($J_{M-R} = 1.45\,cm^{-1}$). The difference can be considered to arise from the difference in the number of carbon and nitrogen atoms on the π-system between the $Ru_2^{II,III}$ unit and the N–O group based on the spin-polarization mechanism. A zig-zag chain structure of alternating $Ru_2^{II,III}$ unit and *m*-nitpy units was also confirmed by the X-ray crystal structure of $[Ru_2(O_2CC_2H_5)_4(m\text{-nitpy})]_n(PF_6)_n$, as in the case of $[Ru_2(O_2CC(CH_3)_3)_4(p\text{-nitpy})]_n(BF_4)_n$. One of axial sites of the $Ru_2^{II,III}$ core is occupied by one of the two N–O groups of *m*-nitpy with the Ru–O distance of 2.295(4) Å and the other site by the pyridyl nitrogen with a Ru–N distance of 2.271(5) Å. The magnetic interaction through the N–O group was estimated to be $J_{M-R} = 5\,cm^{-1}$ and the interaction through the pyridyl group at $J'_{M-R} = -1.7\,cm^{-1}$.

For the ruthenium(II, III) carboxylates with nitroxide radicals, the magnetic interaction and axial bond angle with the nitroxide are strongly correlated. The J_{M-R} and J_{R-R} values and the Ru–O–N angles are listed in Table 4 together with those of the nitroxide complexes of ruthenium(II, II) and rhodium(II, II) carboxylates. The J_{M-R} and J_{R-R} values are plotted against the Ru–O–N angles for the ruthenium(II, III) complexes in Fig. 14. The J_{M-R} and J_{R-R} decrease and increase, respectively, as the Ru–O–N angle increases [89]. When the Ru–O–N angle is around 120°, the J_{M-R} is positive (ferromagnetic), whereas J_{R-R} is negative (antiferromagnetic) as in the case for the rhodium(II, II) nitroxide complexes in Table 4. By considering the overlap

between the σ^* and π^* orbitals of $Ru_2^{II,III}$ core and the π^* orbital of the nitroxide radical, it is understandable that the ferro- and antiferromagnetic interactions are both operative through the same Ru–O_{ax} bond [89].

3. Two- and three-dimensional assemblies

Tetradentate cyano ligands such as tcne are of interest, because they have a potential function of μ_4-bridging, if all of their donor groups work fully. Cotton and Kim reported the first example of the μ_4-bridging to metal–metal bond system [93]. They reacted $Rh_2(O_2CCF_3)_4$ and tcne and obtained $[Rh_2(O_2CCF_3)_4(tcne)]_n$. The crystal structure shows that all four CN groups of tcne function as a μ_4-bridging group to form infinite 2D sheets. Dunbar found a sheet structure consisting of hexagonal rings of Mo_2 dimers connected by μ_4-tcne in $[Mo_2(O_2CC(CH_3)_3)_4(tcne)]_n$ [69]. By using tetradentate bridging ligands such as tcne, we also intended to make two-dimensional assemblies of dinuclear ruthenium carboxylates [75]. However, we could not confirm such a system by X-ray crystallography. Dunbar and co-workers successfully isolated such compounds as $[\{Ru_2(O_2CCF_3)_4\}_2(tcnq)]_n\cdot 3nC_6H_5CH_3$ and $[\{Rh_2(O_2CCF_3)_4\}_2(tcnq)]_n\cdot 3nC_6H_5CH_3$, which are isostructural to each other. All four cyano groups of tcnq are coordinated to the dinuclear metal cores, resulting in a distorted hexagonal 2D network [94]. The bond lengths within the tcnq molecules are intermediate between the values of $tcnq^0$ and $tcnq^-$, indicating partially reduced tcnq.

Perrhenate ion is an interesting anion, having three different coordination modes, monodentate, chelate, and bridging. Jimenez-Aparicio et al. tried to prepare new supramolecular compounds of ruthenium(II, III) carboxylates using the perrhenate ion as a linking ligand [46]. They obtained polymeric compounds $[Ru(O_2CR)_4(ReO_4)]_n$ (R = CH_3, $C(C_6H_5)_2CH_3$, $C(CH_3)_3$, $CH_2CH_2OCH_3$, $C(CH_3)=CHC_2H_5$, C_6H_4-*p*-OCH_3, C_6H_5), where the ReO_4^- ions connect the $Ru_2(O_2CR)_4^+$ units through the axial positions to form one-dimensional linear chains. They analyzed the magnetic susceptibility data of these compounds using Eq. (1) and obtained zJ values from -0.04 to $-1.74\,cm^{-1}$, which can be considered to be very weak according to the presence of $Ru_2^{II,III}$ units connected by diamagnetic tetrahedral perrhenate ions (Table 1).

Kitagawa and co-workers prepared a 2D coordination polymer with a honeycomb (6, 3) network $[\{Ru_2(O_2CC_6H_5)_4\}_3(trz)_2]_n$ (trz = triazine) [53]. In this complex, the $Ru_2^{II,II}$ unit is used as a linear linker motif and triazine as a three-connected node to form a magnetic 2D Kagome lattice. The magnetic data can be fit with the molecular field approximation and $g = 2.0$, $D = 254$, $zJ = -2.2\,cm^{-1}$. They attributed the negative zJ value to the antiferromagnetic interaction due to the spin delocalization mechanism between the $d\pi^*$–$d\pi^*$ orbitals of the Ru_2 cores through the $p\pi^*$ orbital rather than the spin polarization mechanism giving a ferromagnetic interaction between them. The expected spin-frustration in the 2D network was not observed because of the large zero-field splitting effect of the Ru_2 cores.

Ebihara and co-workers treated ruthenium(II, III) pivalate with hexanuclear molybdenum clusters of octacapped octahedra Mo_6X_8 (X = Cl, Br) having six axial halogeno atoms X′ (X′ = Cl, Br) and obtained heterometal complexes $[\{Ru_2(O_2CC(CH_3)_3)_4\}_2\{(Mo_6X_8)X'_6\}]_n$ [95]. This type of cluster can be used as linking ligands for 3D construction with the axial halogeno atoms. However, the X-ray structure analysis showed the 2D sheet of square lattices with molybdenum clusters as corners and ruthenium units as edges, and two axial halogeno atoms remaining as terminal ones.

In order to construct 3D networks, hexacyanometalate ions such as $[Co(CN)_6]^{3-}$ are most promising linking ligands, because they have three-directional coordinating cyano groups. The first attempt to be built in this metal-complex-bridge to metal–metal-bonded dimer was done by Jacobson and co-workers for rhodium acetate using $[Co(CN)_6]^{3-}$ [96]. They obtained purple crystals of $K_{3n}[\{Rh_2(O_2CCH_3)_4\}_2Co(CN)_6]_n$. The structure consists of 2D sheet-like networks where each $[Co(CN)_6]^{3-}$ unit uses four in-plane CN groups to connect $Rh_2^{II,II}$ dimers via Co–CN–Rh bonds. Jun and co-workers applied this $[Co(CN)_6]^{3-}$ bridging unit to the dinuclear ruthenium system [97]. By using $[Ru_2(chp)_4]PF_6$ (chp = 6-chloro-2-hydroxypyridinato), they obtained a pentanuclear complex, $K[\{Ru_2(chp)_4\}_2Co(CN)_6]$, where the two $Ru_2(chp)$ units are bridged by one $Co(CN)_6^{3-}$ in a linear array. The magnetic susceptibility data are similar to that of the chain compound $[Ru_2(O_2CC_3H_7)_4Cl]_n$ [29,33], suggesting the magnetic interaction through the hexacyanocobaltate bridge can be neglected. We examined reactions with $K_3[M(CN)_6]$ (M = Co, Fe) and $K_4[Fe(CN)_6]$ adopting ruthenium(II, III) pivalate as metal–metal-bonded dimer [98]. Reaction of $[Ru_2(O_2CC(CH_3)_3)_4(H_2O)_2]BF_4$ and $K_3[M(CN)_6]$ afforded analytically pure heterometal species $[\{Ru_2(O_2CC(CH_3)_3)_4\}_3(H_2O)M(CN)_6]_n$ (M = Fe and Co) [99]. We successfully isolated these complexes in the crystalline form and revealed the crystal structures, both of which are isostructural (Fig. 15). The $M(CN)_6$ uses four cyano groups to bind four $Ru_2^{II,III}$ units to form a 2D sheet made up of 28-membered $[–M–CN–Ru_2–NC–]_4$ rings as shown in Fig. 16. One of the remaining two cyano groups coordinates to one Ru_2 unit and the other CN group is hydrogen bonded to the axial water molecule bound to the neighboring Ru_2 unit to connect the 2D sheets to form a 3D network (Fig. 17). The magnetic susceptibility data (above 10 K) of $[\{Ru_2(O_2CC(CH_3)_3)_4\}_3(H_2O)Co(CN)_6]_n$ can be fit to the Curie–Weiss expression $\chi_M = C/(T-\theta)$ with $\theta = -23.0$ K. On the other hand, the magnetic moment of $[\{Ru_2(O_2CC(CH_3)_3)_4\}_3(H_2O)Fe(CN)_6]_n$ gradually decreases with decrease of temperature until it abruptly increases at ~20 K reaching $10.34\mu_B$ at 8 K, showing ferrimagnetic behavior due to the antiferromagnetic interaction between the 3/2 spins of the $Ru_2^{II,III}$ dimers and 1/2 spins of $Fe(CN)_6^{3-}$ bridges (Fig. 18). The Curie–Weiss law fit from 100 to 300 K gives a negative Weiss constant, θ, of -34.8 K.

By using ruthenium(II, III) acetate, Miller and co-workers prepared $[\{Ru_2(O_2CCH_3)_4\}_3M(CN)_6]_n$ (M = Cr, Mn, Fe and Co) [49,100]. Air stable $[\{Ru_2(O_2CCH_3)_4\}_3M(CN)_6]_n$ (M = Cr, Fe and Co) were obtained by mixing aque-

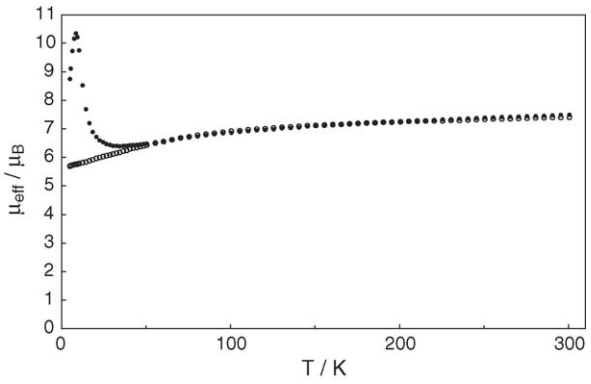

Fig. 18. Temperature dependence of the magnetic moments of $[\{Ru_2(O_2CC(CH_3)_3)_4\}_3(H_2O)Fe(CN)_6]_n\cdot 2nH_2O$ (●) and $[\{Ru_2(O_2CC(CH_3)_3)_4\}_3(H_2O)Co(CN)_6]_n\cdot 2nH_2O$ (◯).

ous solutions of $[Ru_2(O_2CCH_3)_4]Cl$ and $K_3[M(CN)_6]$, while compounds prepared from acetonitrile solution such as $[\{Ru_2(O_2CCH_3)_4\}_3Mn(CN)_6]_n$ are only stable below −20 °C. They proposed a 3D network structure with –M–CN–Ru_2–NC–M– linkages along all three Cartesian axes of the cubic unit cell. The Reitveld analysis of the synchrotron powder diffraction data support the body centered cubic structures. They found similar magnetic behavior to our compounds and introduced the Weiss constant, θ, and the zero-field splitting, D, for the magnetic susceptibility data to account for magnetic interaction between the paramagnetic species:

$$\chi = 3\chi_{Ru_2} + \chi_M \quad (5)$$

where:

$$\chi_{Ru_2} = \{Ng^2\mu_B^2/k(T-\theta)\}[(1/3)[1+9\exp(-2D/kT)]/4\{1 + \exp(-2D/kT)\} + (2/3)[1+(3kT/4D)\{1 - \exp(-2D/kT)\}]/\{1+\exp(-2D/kT)\}] + \text{tip} \quad (6)$$

$$\chi_M = Ng^2\mu_B^2 S(S+1)/3k(T-\theta) \quad (7)$$

The susceptibility data were fit with Eq. (5) with $D = 69.4\,cm^{-1}$, $\theta = -40$ K for $[\{Ru_2(O_2CCH_3)_4\}_3Cr(CN)_6]_n$ (above 120 K), $D = 69.4\,cm^{-1}$, $\theta = 0$ K for $[\{Ru_2(O_2CCH_3)_4\}_3Fe(CN)_6]_n$ (above 15 K), $D = 69.4\,cm^{-1}$, $\theta = 0$ K for $[\{Ru_2(O_2CCH_3)_4\}_3Co(CN)_6]_n$ (above 4 K) $D = 69.4\,cm^{-1}$, $\theta = -20$ K for $[\{Ru_2(O_2CCH_3)_4\}_3Mn(CN)_6]_n$ (above 60 K). The magnetic ordering (2.1–34.5 K) of the $(Ru_2)_3Cr$ (34.5 K), $(Ru_2)_3Fe$ (2.1 K), and $(Ru_2)_3Mn$ (9.6 K) compounds was determined from the real, in-phase (χ') and imaginary, out-of-phase (χ'') ac susceptibilities as well as the zero-field cooled and field cooled magnetization studies. The field dependence of the magnetization data at 2 K for the $(Ru_2)_3Cr$ compound obtained from the aqueous solution showed an unusual constricted hysteresis loop with a coercive field of 470 Oe, while the magnetization data for the $(Ru_2)_3Cr$ from the acetonitrile solution, $(Ru_2)_3Fe$, and $(Ru_2)_3Mn$ compounds showed a normal hysteresis loop with a coercive field of 1670, 10, and 990 Oe, respectively. They analyzed the field-dependent magnetization data of $[Ru_2(O_2CCH_3)_4Cl]_n$ and $[\{Ru_2(O_2CCH_3)_4\}_3Co(CN)_6]_n$ considering the zero-field-splitting effect of the $Ru_2^{II,III}$ units [101]. Further, they studied the pivalate systems by adding $[\{Ru_2(O_2CC(CH_3)_3)_4\}_3Cr(CN)_6]\cdot 2H_2O$ to our compounds [50]. The magnetic susceptibility data were fit with Eq. (5) with $D = 69.4\,cm^{-1}$, $\theta = -45$ K for $[\{Ru_2(O_2CC(CH_3)_3)_4\}_3Cr(CN)_6]_n\cdot 2nH_2O$ (above 150 K), $D = 69.4\,cm^{-1}$, $\theta = -5$ K for $[\{Ru_2(O_2CC(CH_3)_3)_4\}_3Fe(CN)_6]_n\cdot 2nH_2O$ (above 50 K), $D = 69.4\,cm^{-1}$, $\theta = 0$ K for $[\{Ru_2(O_2CC(CH_3)_3)_4\}_3Co(CN)_6]_n\cdot 2nH_2O$ (above 4 K). Magnetic ordering of the $(Ru_2)_3Cr$ and $(Ru_2)_3Fe$ compounds was confirmed by the real and imaginary ac susceptibilities. The former has nearly frequency independent peaks for both $\chi'(T)$ at 37.5 K and $\chi''(T)$ at 36.5 K, while the latter has a slight frequency dependence for both $\chi'(T)$ and $\chi''(T)$ peaks around 4.8 K. The coercive fields are 20,000 and 190 Oe, respectively, which are larger than those of the analogous acetates with the 3D structures. Recently, we have extended these systems using octacyanometalate ions such as $[W(CN)_8]^{3-}$ which might be more interesting and obtained a complex $(PPh_4)_2[Ru_2(O_2CC(CH_3)_3)_4W(CN)_8]_n$ [102]. The X-ray structure analysis reveals an alternating arrangement of Ru_2 units and $[W(CN)_8]^{3-}$ in a 1D chain. The magnetic susceptibility data shows a ferrimagnetic behavior for this complex.

Zheng and co-workers reported the crystal structure of a ruthenium diphosphonate $(NH_4)_{3n}[Ru_2(hedp)_2]_n\cdot 2nH_2O$ (hedp = 1-hydroxyethylidenediphosphonato $CH_3C(OH)(PO_3)_2$) having a 'paddlewheel' core, $Ru_2(hedp)_2$, where the $Ru_2^{II,III}$ units are cross-linked by axial coordination to the neighboring $Ru_2(hedp)_2$ units by one of the uncoordinated phosphonato-oxygen atoms into a 2D network [47]. They obtained magnetic parameters $D = 89.4\,cm^{-1}$, $\theta = 0.72$ K from the susceptibility data (25–300 K) by using Eq. (5). They prepared linear chain compounds with the formula, $Na_{7n}[Ru_2(hedp)_2Fe(CN)_6]_n\cdot 24nH_2O$ and $Na_{4n}[Ru_2(hedp)_2X]_n\cdot 16nH_2O$ (X = Cl, Br) [48]. In the crystal structures, hexacyanoferrate(II) or chloride ions bridge the $Ru_2(hedp)_2$ units to form an alternately arranged linear chain molecule. These chains are connected by hydrogen bonds with the hydroxy groups of hedp moieties, leading to a 3D network structure. The magnetic data of the former compound was fit by Eq. (1) with $D = 101.6\,cm^{-1}$, $zJ = -0.044\,cm^{-1}$, showing a very weak antiferromagnetic interaction between the $Ru_2^{II,III}$ units through the diamagnetic $Fe(CN)_6^{4-}$ bridges.

4. Conclusions

Ruthenium carboxylates with a paddlewheel dinuclear core give various types of axially coordinated dinuclear, tetranuclear, and polynuclear complexes in combination with linking ligands such as *N*,*N*′-bidentate ligands, *p*-quinones, organic electron acceptors with cyano groups, nitroxide radicals, and inorganic hexacyanometalate. The paramagnetic dinuclear units with oxidation state of ruthenium(II, II) (two unpaired electrons located in the $Ru_2^{II,II}$ core) and ruthenium(II, III) (three unpaired electrons in the $Ru_2^{II,III}$ core) are both available for the assembled complexes and have been investigated with respect to their mag-

netic interactions through the linking ligands. The unpaired electrons can magnetically communicate through the linking ligands between the dinuclear units, although the interactions are generally weak. When the linking ligands are paramagnetic, the magnetic interaction between the Ru_2 cores and the linking ligands sometimes become stronger, giving important magnetic properties such as a ferrimagnetic interaction. These results show a high potential for dinuclear ruthenium carboxylates as building blocks for magnetic materials, although there are some problems to be solved, one of which is the strong zero-field splitting, D = ca. 300 and 60 cm^{-1} for $Ru_2^{II,II}$ and $Ru_2^{II,III}$ cores, respectively, leading to a significant decrease in the magnetic moments when the temperature is lowered. We expect that further studies will be devoted to develop their magnetic potential as a unique spin source for new magnetic materials.

Acknowledgments

The present work was partially supported by the "Open Research Center" Project for Private Universities: matching fund subsidy and Grants-in-Aid for Scientific Research Nos. 16550062 and 17550060 from the Ministry of Education, Culture, Sports, Science and Technology.

References

[1] F.A. Cotton, C.A. Murillo, R.A. Walton, Multiple Bonds Between Metal Atoms, 3rd ed., Springer Science and Business Media, New York, 2005.
[2] T.A. Stephenson, G. Wilkinson, J. Inorg. Nucl. Chem. 28 (1966) 2285.
[3] M. Mukaida, T. Nomura, T. Ishimori, Bull. Chem. Soc. Jpn. 40 (1967) 2462.
[4] J.N. van Niekerk, F.R.L. Schoening, Nature 171 (1953) 36.
[5] J.N. van Niekerk, F.R.L. Schoening, Acta Crystallogr. 6 (1953) 227.
[6] M.J. Bennett, K.G. Caulton, F.A. Cotton, Inorg. Chem. 8 (1969) 1.
[7] A.J. Lindsay, R.P. Tooze, M. Motevalli, M.B. Hursthouse, G. Wilkinson, J. Chem. Soc. Chem. Commun. (1984) 1383.
[8] A.J. Lindsay, G. Wilkinson, M. Motevalli, M.B. Hursthouse, J. Chem. Soc. Dalton Trans. (1985) 2321.
[9] A.J. Lindsay, G. Wilkinson, M. Motevalli, M.B. Hursthouse, J. Chem. Soc. Dalton Trans. (1987) 2723.
[10] J.G. Norman, G.E. Renzoni, D.A. Case, J. Am. Chem. Soc. 101 (1979) 5256.
[11] G. Estiu, F.D. Cukiernik, P. Maldivi, O. Poizat, Inorg. Chem. 38 (1999) 3030.
[12] M.A.S. Aquino, Coord. Chem. Rev. 170 (1998) 141.
[13] A.M. Giroud-Godquin, Coord. Chem. Rev. 178–180 (1998) 1485.
[14] T.M. Buslaeva, S.N. Red'kina, O.V. Rudnitskaya, Russ. J. Coord. Chem. 25 (1999) 1.
[15] M.A.S. Aquino, Coord. Chem. Rev. 248 (2004) 1025.
[16] G.G. Briand, M.W. Cooke, T.S. Cameron, H.M. Farrell, T.J. Burchell, M.A.S. Aquino, Inorg. Chem. 40 (2001) 3267.
[17] M.C. Barral, R. Gonzalez-Prieto, R. Jimenez-Aparicio, J.L. Priego, M.R. Torres, F.A. Urbanos, Eur. J. Inorg. Chem. (2003) 2339.
[18] M.C. Barral, R. Gonzalez-Prieto, R. Jimenez-Aparicio, J.L. Priego, M.R. Torres, F.A. Urbanos, Eur. J. Inorg. Chem. (2004) 4491.
[19] W.-Z. Wang, D.-Z. Liao, G.-L. Wang, Fudan Xuebao 42 (2003) 897.
[20] F.A. Cotton, M. Matusz, B. Zhong, Inorg. Chem. 27 (1988) 4368.
[21] E.V. Dikarev, B. Li, J. Cluster Sci. 15 (2004) 437.
[22] Z. Chaia, A. Zelcer, B. Donnio, M. Rusjan, F.D. Cukiernik, D. Guillon, Liq. Cryst. 31 (2004) 1019.
[23] P. Angaridis, F.A. Cotton, C.A. Murillo, X.-P. Wang, Acta Crystallogr. C 61 (2005) m109.
[24] J.S. Valentine, A.J. Silverstein, Z.G. Soos, J. Am. Chem. Soc. 96 (1974) 97.
[25] B. Morosin, R.C. Hughes, Z.G. Soos, Acta Crystallogr. B 31 (1975) 762.
[26] F.A. Cotton, Y. Kim, T. Ren, Inorg. Chem. 31 (1992) 2723.
[27] F.D. Cukiernik, A.-M. Giroud-Godquin, P. Maldivi, J.-C. Marchon, Inorg. Chim. Acta 215 (1994) 203.
[28] E.J. Beck, K.D. Drysdale, L.K. Thompson, L. Li, C.A. Murphy, M.A.S. Aquino, Inorg. Chim. Acta 279 (1998) 121.
[29] J. Telser, R.S. Drago, Inorg. Chem. 23 (1984) 3114;
J. Telser, R.S. Drago, Inorg. Chem. 24 (1985) 4765.
[30] C.J. O'Connor, Prog. Inorg. Chem. 29 (1982) 203.
[31] D. Yoshioka, M. Mikuriya, M. Handa, Bull. Chem. Soc. Jpn. 77 (2004) 2205.
[32] R. Jimenez-Aparicio, F.A. Urbanos, J.M. Arrieta, Inorg. Chem. 40 (2001) 613.
[33] F.D. Cukiernik, D. Luneau, J.-C. Marchon, P. Maldivi, Inorg. Chem. 37 (1998) 3698.
[34] Y. Sayama, M. Handa, M. Mikuriya, R. Nukada, I. Hiromitsu, K. Kasuga, in: G. Ondrejovic, A. Sirota (Eds.), Coordination Chemistry at the Turn of the Century, Slovak Technical University Press, Bratislava, 1999, p. 447.
[35] M.C. Barral, R. Jimenez-Aparicio, D. Perez-Quintanilla, J.L. Priego, E.C. Royer, M.R. Torres, F.A. Urbanos, Inorg. Chem. 39 (2000) 65.
[36] T. Togano, M. Mukaida, T. Nomura, Bull. Chem. Soc. Jpn. 53 (1980) 2085.
[37] A. Bino, F.A. Cotton, T.R. Felthouse, Inorg. Chem. 18 (1979) 2599.
[38] F.A. Cotton, Y. Kim, T. Ren, Polyhedron 12 (1993) 607.
[39] M.C. Barral, R. Jimenez-Aparicio, J.L. Priego, E.C. Royer, M.J. Saucedo, F.A. Urbanos, U. Amador, J. Chem. Soc. Dalton Trans. (1995) 2183.
[40] M.C. Barrel, R. Jimenez-Aparicio, E.C. Royer, C. Ruiz-Valero, M.J. Saucedo, F.A. Urbanos, Inorg. Chem. 33 (1994) 2692.
[41] M.C. Barrel, R. Jimenez-Aparicio, D. Perez-Quintanilla, E. Pinilla, J.L. Priego, E.C. Royer, F.A. Urbanos, Polyhedron 18 (1999) 371.
[42] D. Yoshioka, M. Handa, H. Azuma, M. Mikuriya, I. Hiromitsu, K. Kasuga, Mol. Cryst. Liq. Cryst. 342 (2000) 133.
[43] M. Handa, D. Yoshioka, Y. Sayama, K. Shiomi, M. Mikuriya, I. Hiromitsu, K. Kasuga, Chem. Lett. (1999) 1033.
[44] D. Yoshioka, M. Handa, M. Mikuriya, I. Hiromitsu, K. Kasuga, Mater. Sci. Poland 23 (2005) 765.
[45] H. Miyasaka, R. Clerac, C.S. Campos-Fernandez, K.R. Dunbar, Inorg. Chem. 40 (2001) 1663.
[46] G. Arribas, M.C. Barral, R. Gonzalez-Prieto, R. Jimenez-Aparicio, J.L. Priego, M.R. Torres, F.A. Urbanos, Inorg. Chem. 44 (2005) 5770.
[47] X.-Y. Yi, L.-M. Zheng, W. Xu, S. Feng, Inorg. Chem. 42 (2003) 2827.
[48] X.-Y. Yi, B. Liu, R. Jimenez-Aparicio, F.A. Urbanos, S. Gao, W. Xu, J.-S. Chen, Y. Song, L.-M. Zheng, Inorg. Chem. 44 (2005) 4309.
[49] T.E. Vos, Y. Liao, W.W. Shum, J.-H. Her, P.W. Stephens, W.M. Reiff, J.S. Miller, J. Am. Chem. Soc. 126 (2004) 11630.
[50] T.E. Vos, J.S. Miller, Angew. Chem. Int. Ed. 44 (2005) 2416.
[51] M. Handa, D. Yoshioka, M. Mikuriya, I. Hiromitsu, K. Kasuga, Mol. Cryst. Liq. Cryst. 376 (2002) 257.
[52] H. Miyasaka, R. Clerac, C.S. Campos-Fernandez, K.R. Dunbar, J. Chem. Soc. Dalton Trans. (2001) 858.
[53] S. Furukawa, M. Ohba, S. Kitagawa, Chem. Commun. (2005) 865.
[54] F.A. Cotton, Y. Kim, T. Ren, Inorg. Chem. 31 (1992) 2608.
[55] M. Handa, M. Yasuda, Y. Muraki, D. Yoshioka, M. Mikuriya, K. Kasuga, Chem. Lett. 32 (2003) 946.
[56] J.L. Wesemann, M.H. Chisholm, Inorg. Chem. 36 (1997) 3258.
[57] V.M. Miskowski, T.M. Loehr, H.B. Gray, Inorg. Chem. 26 (1987) 1098.
[58] V.M. Miskowski, H.B. Gray, Inorg. Chem. 27 (1988) 2501.
[59] F.A. Cotton, E. Pedersen, Inorg. Chem. 14 (1975) 399.
[60] T.P. Zhu, M.Q. Ahsan, T. Malinski, K.M. Kadish, J.L. Bear, Inorg. Chem. 23 (1984) 2.
[61] F.A. Cotton, E. Pedersen, Inorg. Chem. 14 (1975) 388.
[62] S.L. Schiavo, G. Bruno, P. Zanello, F. Laschi, P. Piraino, Inorg. Chem. 36 (1997) 1004.

[63] M.E. Peover, J. Chem. Soc (1962) 4540.
[64] M.C. Barral, R. Gonzalez-Prieto, R. Jimenez-Aparicio, J.L. Priego, M.R. Torres, F.A. Urbanos, Inorg. Chim. Acta 358 (2005) 217.
[65] S. Furukawa, S. Kitagawa, Inorg. Chem. 43 (2004) 6464.
[66] J.S. Miller, A.J. Epstein, W.M. Reiff, Chem. Rev. 88 (1988) 201.
[67] L. Ballester, A. Gutierrez, M.F. Perpinan, M.T. Azcondo, Coord. Chem. Rev. 190–192 (1999) 447.
[68] R. Kato, Bull. Chem. Soc. Jpn. 73 (2000) 515.
[69] K.R. Dunbar, J. Cluster Sci. 5 (1994) 125.
[70] J.-M. Giraudon, J.-E. Guerchais, J. Sala-Pala, L. Toupet, J. Chem. Soc. Chem. Commun. (1988) 921.
[71] S.L. Bartley, K.R. Dunbar, Angew. Chem. Int. Ed. Engl. 30 (1991) 448.
[72] K.R. Dunbar, X. Quyang, Mol. Cryst. Liq. Cryst. 273 (1995) 21.
[73] S.C. Huckett, C.A. Arrington, C.J. Burns, D.L. Clark, B.I. Swanson, Synth. Met. 41–43 (1991) 2769.
[74] D. Li, S.C. Huckett, T. Frankcom, M.T. Paffett, J.D. Farr, M.E. Hawley, S. Gottesfeld, J.D. Thompson, C.J. Burns, B.I. Swanson, in: T. Bein (Ed.), Supramolecular Architecture: Synthetic Control in Thin Films and Solids, Proceedings of the American Chemical Society Symposium Series 499, Washington, DC, 1992 (Chapter 4).
[75] D. Yoshioka, M. Handa, M. Mikuriya, K. Kasuga, in: M. Melnik, J. Sima, M. Tatarko (Eds.), Advances in Coordination, Bioinorganic and Inorganic Chemistry, Slovak Technical University Press, Bratislava, 2005, p. 218.
[76] F.A. Cotton, T.R. Felthouse, Inorg. Chem. 21 (1982) 2667.
[77] T.-Y. Dong, D.N. Hendrickson, T.R. Felthouse, H.-S. Shieh, J. Am. Chem. Soc. 106 (1984) 5373.
[78] T.R. Felthouse, T.-Y. Dong, D.N. Hendrickson, H.-S. Shieh, M.R. Thompson, J. Am. Chem. Soc. 108 (1986) 8201.
[79] A. Cogne, A. Grand, P. Rey, R. Subra, J. Am. Chem. Soc. 109 (1987) 7927.
[80] A. Cogne, A. Grand, P. Rey, R. Subra, J. Am. Chem. Soc. 111 (1989) 3230.
[81] A. Cogne, E. Belorizky, J. Laugier, P. Rey, Inorg. Chem. 33 (1994) 3364.
[82] M. Handa, Y. Sayama, M. Mikuriya, R. Nukada, I. Hiromitsu, K. Kasuga, Bull. Chem. Soc. Jpn. 68 (1995) 1647.
[83] M. Handa, Y. Sayama, M. Mikuriya, R. Nukada, I. Hiromitsu, K. Kasuga, Chem. Lett. (1996) 201.
[84] M. Handa, Y. Sayama, M. Mikuriya, R. Nukada, I. Hiromitsu, K. Kasuga, Bull. Chem. Soc. Jpn. 71 (1998) 119.
[85] Y. Sayama, M. Handa, M. Mikuriya, I. Hiromitsu, K. Kasuga, Chem. Lett. (1998) 777.
[86] Y. Sayama, M. Handa, M. Mikuriya, I. Hiromitsu, K. Kasuga, Chem. Lett. (1999) 453.
[87] Y. Sayama, M. Handa, M. Mikuriya, I. Hiromitsu, K. Kasuga, Bull. Chem. Soc. Jpn. 73 (2000) 2499.
[88] Y. Sayama, M. Handa, M. Mikuriya, I. Hiromitsu, K. Kasuga, Bull. Chem. Soc. Jpn. 74 (2001) 2129.
[89] Y. Sayama, M. Handa, M. Mikuriya, I. Hiromitsu, K. Kasuga, Bull. Chem. Soc. Jpn. 76 (2003) 769.
[90] M. Handa, Y. Sayama, M. Mikuriya, I. Hiromitsu, K. Kasuga, Mater. Sci. 21 (2003) 199.
[91] M. Mikuriya, K. Tanaka, M. Handa, I. Hiromitsu, D. Yoshioka, D. Luneau, Polyhedron 24 (2005) 2658.
[92] O. Kahn, Molecular Magnetism, VCH Publishers, New York, 1993.
[93] F.A. Cotton, Y. Kim, J. Am. Chem. Soc. 115 (1993) 8511.
[94] H. Miyasaka, C.S. Campos-Fernandez, R. Clerac, K. Dunbar, Angew. Chem. Int. Ed. 39 (2000) 3831.
[95] T. Sugiura, K. Ota, M. Ebihara, T. Kawamura, C.R. Chimie 8 (2005) 1760.
[96] J. Lu, W.T.A. Harrison, A.J. Jacobson, Chem. Commun. (1996) 399.
[97] Y. Kim, K.-T. Youm, M.-J. Jun, Bull. Kor. Chem. Soc. 19 (1998) 1023.
[98] D. Yoshioka, M. Mikuriya, M. Handa, Proceedings of the 50th Symposium on Coordination Chemistry of Japan, Kusatsu, 2000, Abst. 1B-B02.
[99] D. Yoshioka, M. Mikuriya, M. Handa, Chem. Lett. (2002) 1044.
[100] Y. Liao, W.W. Shum, J.S. Miller, J. Am. Chem. Soc. 124 (2002) 9336.
[101] W.W. Shum, Y. Liao, J.S. Miller, J. Phys. Chem. A 108 (2004) 7460.
[102] D. Matoga, M. Mikuriya, M. Handa, J. Szklarzewicz, Chem. Lett. 34 (2005) 1550.